DEPARTAMENTO DE ZOOLOGIA

FACULDADE DE CIÊNCIAS E TECNOLOGIA
UNIVERSIDADE DE COIMBRA

Establishment of primary cell cultures from lung tissue biopsies and study of the cellular metabolic responses to cisplatin and radiation exposure

Dissertação apresentada à Universidade de Coimbra para cumprimento dos requisitos necessários à obtenção do grau de Mestre em Biologia Celular e Molecular. O trabalho foi realizado sob a orientação científica da Professora Doutora Isabel Marques Carreira (Laboratório de Citogenética e Genómica da Faculdade de Medicina da Universidade de Coimbra) e da Doutora Iola Duarte (Laboratório associado CICECO Universidade de Aveiro) e supervisão da Professora Doutora Emília Duarte (Faculdade de Ciências e Tecnologia da Universidade de Coimbra).

Ana Filipa Ferreira Ladeirinha

2011

Agradecimentos

À Professora Doutora Isabel Marques Carreira, orientadora deste trabalho, o meu mais sincero agradecimento por todo o apoio, orientação científica, pedagógica e análise crítica desta tese, assim como a cedência das infra-estruturas e equipamentos fundamentais para a realização deste trabalho.

À Doutora Iola Duarte, co-orientadora deste trabalho, quero agradecer por todo o apoio, orientação científica, pedagógica e análise crítica desta tese.

À Professora Doutora Lina Carvalho, por todo o apoio, disponibilidade, orientação científica, pedagógica e análise crítica desta tese.

À Professora Doutora Emília Pedrosa Duarte, coordenadora do Mestrado em Biologia Celular e Molecular, por todo o seu apoio e disponibilidade constantes durante a elaboração desta tese.

A toda a equipa do Laboratório de Citogenética pelos ensinamentos e transmissão de conhecimentos e, sobretudo, pelo carinho e incentivo.

A toda a equipa do Laboratório associado CICECO pela transmissão de conhecimentos e, sobretudo, pela amizade e incentivo.

Às amigas e colegas Rute e Andreia, pela amizade, confiança e apoio durante a realização deste trabalho.

À minha grande amiga Sónia pela presença constante, amizade, apoio e incentivo para prosseguir com este trabalho sem desanimar.

Aos meus pais. Por tudo, por sempre e para sempre.

Ao Pedro, por todo o carinho, força, coragem, apoio, e por estar sempre presente.

.

List of abbreviation

Array- CGH- Array Comparative Genomic Hybridization

ATCC- American Type Culture Collection

ATP- Adenosine Triphosphate

BEZ- Bezafibrate

CDDP- Cisplatin

Cho- Choline

DA- Discriminant Analysis

DMEM- Dulbecco's Modified Eagle Medium

DNA- Desoxiribonucleic Nucleic Acid

D_2O- Deuterated Water

EDTA- Ethylenediaminetetraacetic Acid

EMT- Epithelium Mesenquimal Transistion

FBS- Fetal Bovine Serum

FDA- Food and Drug Administration

FISH- Fluorescent *in situ* Hybridization

Glut- Glutamate

Gly- Glycine

Gln- Glutamine

GSH- Glutathione

GPC- Glycerophosphocholine

GTG- Giemsa-Trypsin-Giemsa

Gy- Gray

HGF- Human Growth Factor

HRMAS- High-Resolution Magic Angle Spinning

Iso- Isoleucine

K- Kelvin

KCL- Potassium Chloride

Leu- Leucine

Mb- Megabases

MNPs- Marine Natural Products

MPA- Medroxyprogestrone Acetate

MTT- (3-4,5-dimethylthiazol-2-yl) 2,5-diphenyl tetrazolium bromide

NAD^+ - Nicotinamide Adenine Dinucleotide

Neg- Negative

NMR- Nuclear Magnetic Resonance

NSCLC- Non-Small-Cell Lung Cancer

PBS- Phosphate Buffer Solution

PCA- Principal Components Analysis

PC- Principal Component

Phe- Phenylalanine

PLS- Partial Least Squares

PLS-DA- Partial Least Squares Regression Discriminant Analysis

PME- Phosphomonoesters

Posit- Positive

SCLC- Small Cell Lung Cancer

SCC- Squamous Cell Carcinoma

s- Seconds

TCA- Tricarboxylic Cycle

tDDP- Transpaltin

Thr- Threonine

TSP- Trimethylsilyl Propionate

TOCSY- Total Correlation Spectroscopy

Tyr- Tyrosine

Urd- Uridine

Val- Valine

Index

Index of Figures

Index of Tables

Abstract

The present work comprises two main parts: (i) the tentative establishment of primary cultures of lung carcinomas and parenchyma obtained from specimens and their cytogenetic and phenotype characterization; (ii) the metabolic characterization of the lung tumor cell line A549 and of its response to different external stimuli, namely a chemotherapy agent (cisplatin) and ionizing radiation. By identifying the metabolites (and related metabolic pathways) which content varies with drug or radiation exposure, it is intended to determine the main perturbations induced in the cells metabolism by those external stimuli. This is performed by means of ^{1}H High Resolution Magic Angle Spinning (HRMAS) NMR spectroscopy (500 MHz). Multivariate analysis methods are used to infer on the relative relevance of the cellular metabolic changes detected by the NMR experiments. In what concerns the first part of this work it was not possible to establish single primary culture cells from surgical specimens, representing the different histological types.

Regarding the metabolic profiling of A549 lung cells by ^{1}H NMR spectroscopy the present study gave some interesting insights concerning the metabolic response of these cells to incubation, and exposure either to CDDP or 6 Gy ionizing radiation. It was found that within the first hours of exposure to CDDP, the cells are able to increase the uptake of glutamine probably in an attempt of overcome the oxidative stress promoted by the drug. At the same time, production of NAD and NADP metabolites are probably increased as judged by the reduction of the niacinamide level. Moreover, in view of guaranteeing the energetic requirements the levels of the ATP and GTP precursors inosine and adenosine are enhanced as well as protein catabolism.

In what concerns the effect of radiation, it was apparent that, after the initial impact observed at 2 hours after irradiation, with changes in a range of metabolites, the cells were able to recover from the effects of the radiation in the subsequent times.

.

Resumo

O presente trabalho compreende duas partes principais: (i) a tentativa de estabelecimento de culturas primárias de carcinomas pulmonares e parênquima obtido a partir de amostras celulares e sua caracterização citogenética e fenotípica. (ii) A caracterização metabólica da linha celular do tumor de pulmão A549 e da sua resposta a diferentes estímulos externos, ou seja, um agente de quimioterapia (cisplatina) e radiação ionizante. Ao identificar os metabólitos (e vias metabólicas relacionadas) variando com drogas ou exposição a radiação, pretende-se determinar as principais perturbações induzidas no metabolismo das células por aqueles estímulos externos. O estudo é realizado por meio de ^{1}H de alta resolução Angle Spinning Magia (HRMAS) espectroscopia de RMN (500 MHz). Métodos de análise multivariada são utilizados para inferir sobre a relevância relativa das mudanças metabólicas celulares evidências pelas experiências de RMN. No que diz respeito à primeira parte deste trabalho não foi possível estabelecer culturas primárias de células representativas dos espécimes cirúrgicos.

Relativamente ao perfil metabólico da linha celular do pulmão A549, por espectroscopia de by ^{1}H NMR, o presente estudo forneceu alguns dados interessantes sobre a resposta metabólica destas células à exposição a 50 μM CDDP ou radiação ionizante de 6 Gy. Verificou-se que nas primeiras horas de exposição à CDDP, as células são capazes de aumentar a captação de glutamina, provavelmente, numa tentativa de superar o stress oxidativo promovido. Ao mesmo tempo, a produção dos metabolitos NAD e NADP são, provavelmente aumentados devido à redução do nível de niacinamida. Além disso, com vista a garantir os requisitos energéticos os níveis dos precursores de ATP e GTP, inosina e adenosina, são aumentados, bem como o catabolismo protéico.

O efeito da radiação não evidenciou alterações tão bem definido como as encontradas para o efeito da exposição CDDP. Contudo, os resultados parecem apontar para que a célula é capaz de recuperar eficazmente dos efeitos da radiação nas 2h após a exposição.

Aims

1. Aims of this work

It is known that lung cancer is one of the biggest health problems of our days, and the overall cure rate for lung cancer remains too low. One major reason is related to the difficulty in the early detection of the disease. Thus, the development of techniques for the routine study of *in vitro* transformed cells, in different states of transformation, is of particular relevance to therapeutical research.

The present work comprises two main parts:

1. The tentative establishment of primary cultures of lung carcinomas and parenchyma obtained from surgical specimen and their cytogenetic and phenotype characterization. The establishment of primary cultures allows performing the subsequent experiments in controlled conditions, thus allowing the performance of a great number of experiments using the same sample conditions.
2. The metabolic characterization of the lung tumor cell line A549 and of its response to different external stimuli, namely a chemotherapy agent (cisplatin) and ionizing radiation. By identifying the metabolites (and related metabolic pathways) varying with drug or radiation exposure, it is intended to determine the main perturbations induced in the cells metabolism by those external stimuli. This is performed by means of ^{1}H High Resolution Magic Angle Spinning (HRMAS) NMR spectroscopy (500 MHz). Multivariate analysis methods are used to infer on the relative relevance of the cellular metabolic changes detected by the NMR experiments.

Introduction

2. Introduction

2.1 General concepts about cancer biology and lung cancer

Worldwide, about 100 to 350 in 100,000 people die every year due to cancer. Cancer is a disease associated to failures in the mechanisms that control the cell growth and proliferation (Lodish *et al.*, 2004). Legend tells us that Hippocrates, was the first to use the words "cancer" and "carcinoma" (in Greek, *Karkinos* and *Karkinoma*), terms that are the images of an aggressive crap traps that eat their victims (Santoro, 2005). The use of these terms, by the doctors of the classical world, reflected the idea that malignant neoplasms start with a life independent of the human body that supports it (Azevedo, 1996). Formation of cancer involves the coupling of different cellular processes, which are compiled in Figure 1 (Lodish *et al.*, 2004) and will be discussed briefly below.

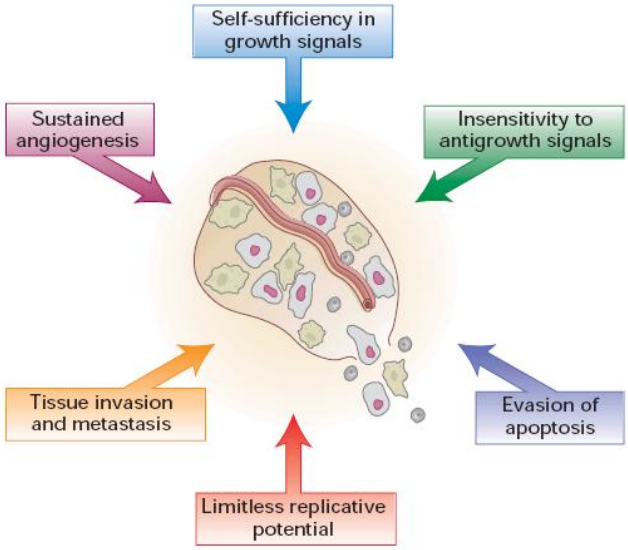

Figure 1: Overview of changes in cells that cause (adapted from Lodish *et al.*, 2004)

Tumor formation is frequently a life-time process that occurs very frequently in older individuals. Fortunately in most cases, a tumor does not represent a great risk to its host as long as it remains well localized and of small size. These tumors are commonly named as benign ones. However, in some cases the deregulation of the processes controlling cell growth and proliferation couple with deregulations on the processes controlling cellular differentiation and apoptosis (cell death process). The coupling of these two deregulations leads to oversized cell agglomerates that easily become malignant tumors. In addition, these cell agglomerates frequently induce the

formation of new blood vessels in order to maintain the tumor oxygenated. This process is named angiogenesis (Lodish *et al.,* 2004). As these malignant tumors develop, the cells may invade surrounding tissues, enter the circulatory system and establish secondary areas of proliferation, called metastasis. In short, what distinguishes a tumor of being benign or malignant, beyond the histomorphological characteristics, is its continued uncontrolled growth and invasion of surrounding healthy tissue capacities (Lodish *et al.,* 2004; DeVita and Rosenberg, 2005).

Oncogenesis, tumorigenesis or carcinogenesis are general terms used to designate the process that leads to a cancer formation. This process may be induced by inherited genetic changes, originating hereditary cancers, or by environmentally promoted mutations, giving rise to sporadic cancers. The genetic errors may only occur in the somatic cells, which by cellular division pass the error to the "daughter" cells, giving rise to a clone of altered cells (Figure 2). However, it is important to keep in mind that rarely a single gene mutation leads to cancer initiation. More typically, cancers are caused by the conjugation of diverse mutations that result from chromossomic changes, such as translocations, amplifications, deletions or epigenetic processes. In fact, cancer is a multifactorial disease, resulting from the interaction between genetic and environmental factors (Croce, 2008 a; Lodish *et al.,* 2004; Pitot, 1993).

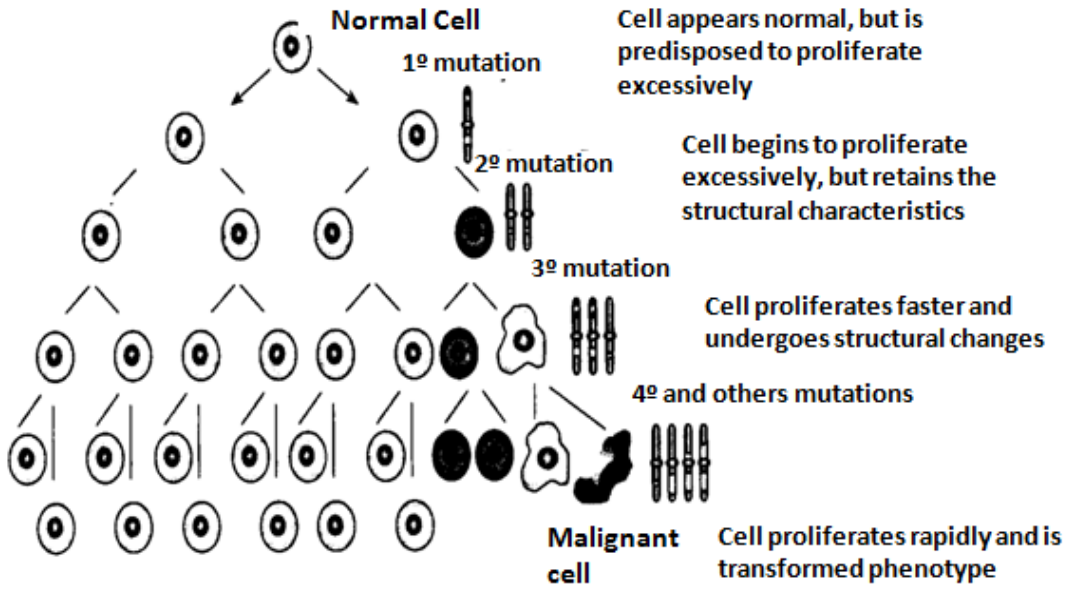

Figure 2: Diagram illustrating the accumulation of mutations, until the appearance of the malignant phenotype (from http://evunix.uevora.pt/~sinogas/TRABALHOS/2001/Imuno01_desord_linfo.htm)

The first evidence that cancer arises from genetic changes came from the studies of Burkitt's lymphomas (Croce, 2008 a). These studies confirm that the simultaneous occurrence of different

mutations is necessary for the occurrence of malignant cellular transformations (Pollock *et al.*, 2006). The proto-oncogenes (which are genes of normal cells) appear to be the targets for chemical carcinogens. These genes control cell proliferation and differentiation and, when mutated, they are able to transform cells *in vitro* (Croce, 2008 b). The abnormal expression of the genes involved in the transcription or transmission of *stimuli* involved in cell growth are called oncogenes (*eg*., ras, fos and src genes) may lead to excessive cell proliferation and to their malignant transformations. Other genes are responsible for the negative control of cell growth and, thus, are called tumor suppressor genes (*eg.*, Rb and p53 genes). When these genes are suppressed and/or under-expressed there is a failure of cell growth control. As easily understandable, this control loss typically occurs only when both copies of the tumor suppressor gene are simultaneously inactivated. This may occur for instance by DNA methylation. In short, the imbalances in the expression of the genes controlling cell growth (stimulators and inhibitors) promote and enhance the cellular transformation processes. (Lodish *et al.*, 2004; Pollock *et al.*, 2006; Pitot, 1993).

Apoptosis, that as referred previously refers to the programmed cell death, is an important process of elimination of damaged cells (*eg.*, cells with mutated DNA). If this process is by any way altered a cancer may be formed. The temporal rate of mitotic division a cell can undergo is dependent on the type of cells. In addition, this process is controlled by many factors, such as the length of telomeres, the activity of tumor suppressor genes and the expression of receptors that trigger apoptosis (*eg*., Fas). When a cell divides, it loses small portions of the ends of chromosomes, which are called telomeres (regions with repeated base pairs that do not encode any important gene for cell survival). Naturally, the cells may avoid the death by promoting the growth of the telomeres by the action of telomerase. The tumor suppressor gene p53 can trigger apoptosis in cells with DNA damage, so individuals with a homozygous loss of this gene are more susceptible to cancer development due to the accumulation of DNA damage. Other genes, such as bcl-2, inhibit apoptosis when expressed excessively. This phenomenon has been pointed as one of the factors leading to chemotherapy resistance (Lodish *et al.*, 2004; Croce, 2008 b).

Several studies have shown that carcinogenesis has three main steps: initiation, promotion and progression (Vincent and Gatenby, 2008). The initiation step may start after the exposure to mutagens, of chemical, physical or biological origin, which promote slight changes in the genetic material of the normal cell. Although not observable on the cell or tissue morphology, those changes may lead to an enhancement of the cellular susceptibility to develop cancer. The gene translocations and mutations may occur during the two first steps (initiation and progression), whereas their amplification occurs during the progression step (Croce, 2008 a).

In the early 20th century lung cancer was a rare disease. However, with the exposure to new etiologic agents and the increase in life expectancy, it became the scourge of this century (Alberg

and Samet, 2003). Nowadays, lung cancer is one of the major cancer-related causes of death in both genders, (Pollock *et al.*, 2006). In this context, the knowledge of the molecular and cellular factors that predispose an individual to the development of this type of cancer is of particular interest (Sun *et al.*, 2007).

It was at the Aspen Lung Conference in 1986 that the cellular and molecular biology of lung cancer were referred for the first time by the scientific community (Pollock *et al.*, 2006). Lung cancer clinicopathology is divided into two main categories: the SCLC (small cell lung cancer) and NSCLC (non-small-cell lung cancer). The NSCLC class may be divided further into three main types: 1) SCC (squamous cell carcinoma), 2) adenocarcinoma, and 3) large cell carcinoma. Beyond the two main categories of lung cancer, a third category is usually considered, which comprise the rare forms of the disease (Sun *et al.*, 2007). The relative incidence of the three lung cancer categories (SCLC, NSCLC and rare forms) is presented in Table 1. The majority of malignant tumors is of carcinomas-type and form in the bronchial epithelium. Moreover, there seems to be an increase of the adenocarcinoma type's incidence in opposition to the decrease tendency observed for the incidence of the SCC-type (Pollock *et al.*, 2006; Sun *et al.*, 2007).

Table 1: Relative incidence of the three pathological types of lung cancer (adapted from Pollock *et al.*, 2006)

Categories	Types	% of incidence
SCLC	___	20-25
NSCLC	SCC	30-35
	Adenocarcinoma	25-30
	Large cell carcinoma	10
Rare forms	____	1

Many studies seem to indicate that tobacco is the main cause of lung cancer. According to Dubey and Powell, about 10-15% of smokers develop lung cancer (Dubey and Powell, 2008). This cause-effect association seems to be more evident for the SCLC- and SCC-types than for adenocarcinoma (Sun *et al.*, 2007). However, other statistics indicate that 15% of lung cancers in men and 53% in women are not smoking-related (Parkin *et al.*, 2005).

Epidemiological studies have identified several factors as promoters of lung cancer. These range from environmental to genetic, hormonal, viral and epigenetic factors (Sun *et al.*, 2007). For nonsmokers, the environmental factors, such as contact with asbestos, chromium, arsenic, cadmium, nickel and silica, and high degrees of pollution, are considered strong promoters for

lung. Neverthless, other lung diseases and diet seem to be also implicated in development of this type of cancer (Sun *et al.,* 2007; Boffetta, 2006).

For all these considerations, the evaluation of the characteristics of tumor tissues as a function of the genetic and nongenetic factors underlying their formation is of particular importance as it may help in the understanding of the etiology of lung cancer. The recognition of potential biomarkers is of utmost relevance for studying the tumor molecular epidemiology (Reid *et al.,* 2008).

2.2 Primary cell cultures as a tool in oncology studies

The tissue cultures techniques were developed in the early twentieth century, by the work of Ross Granville Harrison (1907). This researcher cultured for the first time frog neuronal tissue *in vitro.* Since then, the technique has been applied to cultures of different types of tissues, ranging from animals, including humans, to plants (Gomes, 2007).

Basically there are three main methods of tissue culture as schematized in Figure 3 (Gomes, 2007):

1. Culture of organs, which involves maintaining the three-dimensional architecture characteristic of tissue *in vivo*.
2. Culture of primary cells, in which a fragment of tissue removed directly from an organism, with or without initial step of cell division, is placed at the interface glass (or plastic) / liquid and where, after accession takes place, the migration is promoted in terms of solid substrate. Normally, survival is time-limited.
3. Culture of cells that involves the breakdown (mechanical or enzymatic) of native tissue. Cells are grown in adherent layer, a solid substrate or suspended in culture medium.

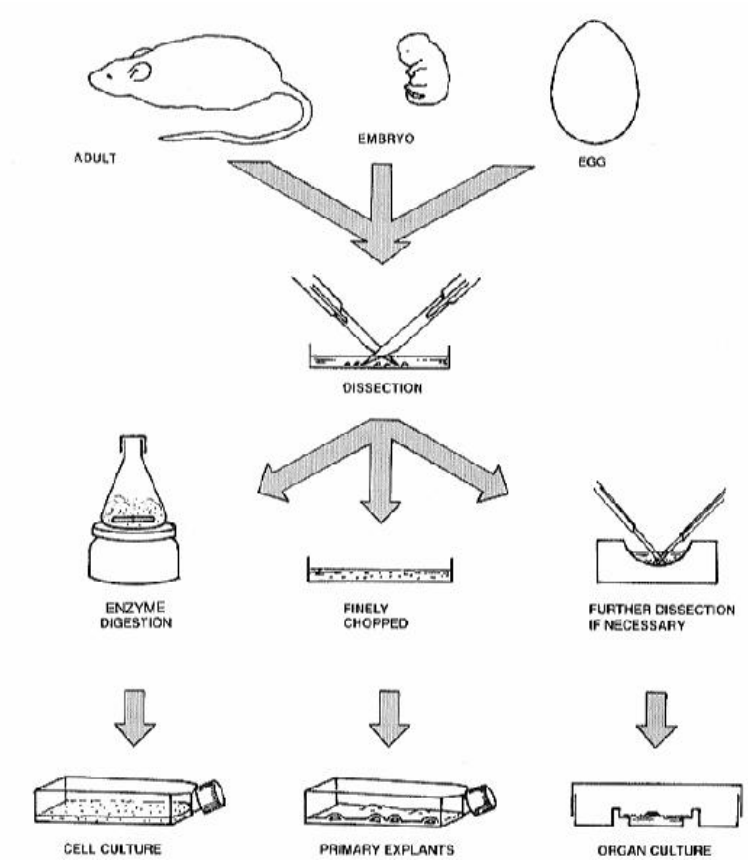

Figure 3: Types of tissue culture (adapted from Gomes, 2007)

Obtaining primary cultures from tissues or organs requires special care. For instance, the material used must be in aseptic conditions, and the cells must be rapidly immersed in the culture medium in order to maintain their viability. The first step consists in disrupting the extracellular matrix and the intercellular junctions that hold cells together. This can be achieved by mechanical dissociation, proteolytic enzymes (collagenase and trypsin) or other disrupting chemical agents (*eg.*, ethylenediaminetetraacetic acid, EDTA). Large cells are separated from the smaller ones and denser cells from non-dense ones by fractional centrifugation. The secondary cultures are obtained from the primary ones by subculturing repeatedly over time *in vitro.* It is, however, important to note that the number of divisions a cell culture can undergo is variable, and depends on both cell type and culture condictions (Gomes, 2007).

As for other tumors, the development of lung cancer is still a multistep process, the nature of which is still not fully understood. The development of routine techniques that isolate and maintain the transformed cells, especially at their early stages of transformation, are of particular importance in this research area. In the last decades, great improvements were achieved in this field. The

determination of biomarkers for lung cancer, for instance, constitutes a great step for the early detection of the disease (Wu, 2004).

2.3 Cytogenetic analysis

Genetic derives from the Greek term *gen*, a term that has been used for the first time in 1906 by Bateson, to describe the variations promoted by heredity (Bernardo, 1982). Genetics comprises several branches, one of the most relevant in health being cytogenetics. The main goal of this branch is the establishment of the relationships between the number and morphology of chromosomes and the phenotype observed in the individual (Robertis and Robertis, 1987).

The use of cytogenetic studies increased exponentially during the first two decades of the second half of the 20^{th} century. These studies allowed the establishment of the elementary foundations of conventional cytogenetics. It was found, for instance, that an hypotonic treatment of cell cultures leads to a chromossomic spreading in metaphase. Moreover, colchicine, was found to block the normal cell division by interfering with the formation of the microtubes. In this way, colchicine became a widely used blocking agent used in cytogenetic studies, as it increases the number of metaphases for microscopic analysis (Patrinos and Ansorge, 2005). Great achievements were reached in what concerns the staining techniques for microscopy analysis. One of the most widely used staining techniques is the GTG (Giemsa-Trypsin-Giemsa). This consists in the incubation with the proteolytic enzyme trypsin and staining with Giemsa. By this way, in the bright field microscope the areas of heterochromatin appear as dark bands while the light bands observed are related to euchromatin, as shown for the normal cells in Figure 4 (Robertis and Robertis, 1987).

The conventional cytogenetic techniques allow the detection of numerical and structural abnormalities as for example exchange of segments between chromosome as in translocation, inversion or gain and/or loss of parts or of entire chromosomes. One of the main limitations of these studies is related to the resolution achieved with classical cytogenetic techniques. In general the resolution is limited to 550 bands, and by this way the structural changes that may be identified must have between 3-5 Mb length. Moreover, recognition of alterations involving the subtelomeric regions of the chromosomes is difficult as these regions are usually related to the light bands observed (Lam *et al.*, 2006).

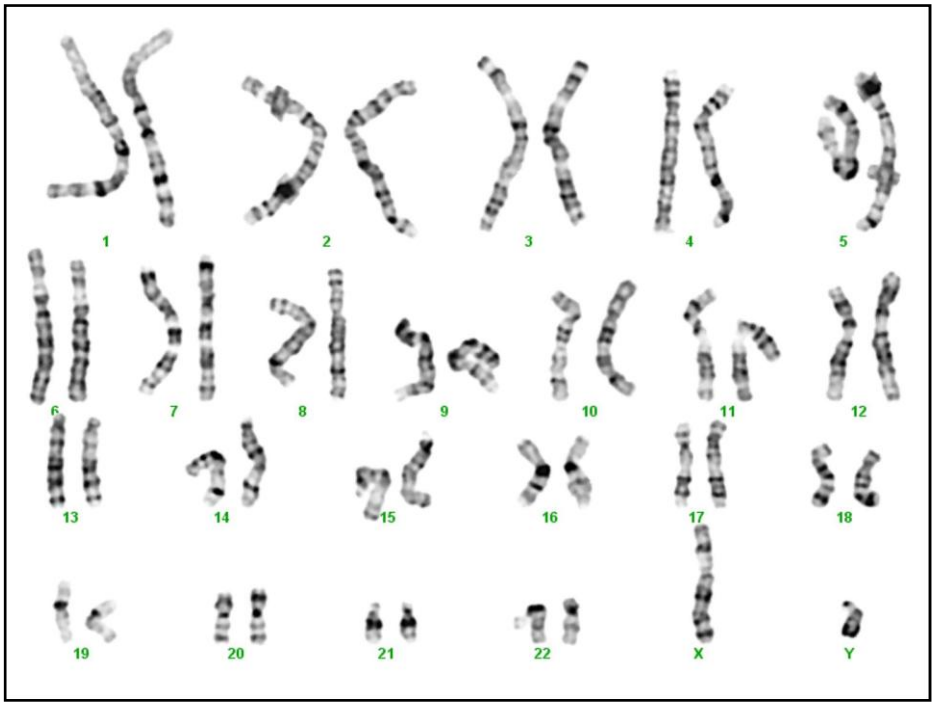

Figure 4: G-banded karyotype of a normal male

2.4 Metabolic studies of cells by Nuclear Magnetic Resonance (NMR) spectroscopy

2.4.1 Principles of NMR spectroscopy

The physical phenomenon behind Nuclear Magnetic Resonance (NMR) spectroscopy was firstly reported in 1946 and it has since then been successfully used in different research areas (Cox *et al.*, 2006). The NMR effect is based on the fact that nuclei of atoms have magnetic properties that can be used to explore some chemical information. From a quantum mechanical point of view, subatomic particles (namely, protons, neutrons and electrons) have spin. In some atoms, such as ^{12}C, ^{16}O, ^{31}S among others, these spins are paired and cancel each other out. As a result, the atom has no overall spin. However, in other atoms (*eg.*, ^{1}H, ^{13}C, ^{31}P, ^{15}N, ^{9}F etc) the nucleus does possess an overall spin. When a sample containing these nuclei are submitted to an external high-intensity magnetic field B_0 the nuclear spins assume certain orientations, the number of which are determined by the spin number I as 2I+1. Thus, in the case of nuclei presenting I = ½, such as ^{1}H, only two orientations are possible in which the nuclear magnetic moment will align either parallel or anti-parallel to the external magnetic field (Figure 5). These two possible relative orientations are often distinguished by the α and β notation, respectively, being the former the energetically favored one (Gil *et al.*, 1987).

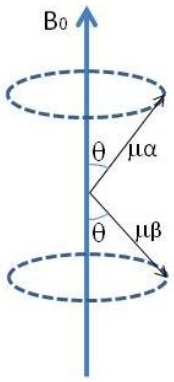

Figure 5: Precession of nuclear magnetic moment μ (for a nucleus with I = ½, γ>0) around the applied field B_0 (adapted from Claridge, 1999)

In practice, when a sample is irradiated with an electromagnetic radiation of correct energy (as determined by its frequency) the nuclei presenting the low-energy spin orientation can be induced to transit to the higher-energy orientation. This is the basis of the NMR effect, for which radio-frequency radiation is used (Vinje and Sletten, 2007). Each NMR signal results from the difference between the energy absorbed by the spins that transit to higher-energy levels and the energy emitted when they return to lower-energy levels.

NMR spectroscopy has enjoyed an exceptional development during the last decades, particularly in what concerns the magnets with increased field strength, the cryogenically cooled probes (to reduce the thermal noise) and the shielding magnets. In the early days of NMR, the technique was mainly used in the pharmaceutical industry as an analytical tool to validate and identify compounds being synthesized by medical chemists (Vinje and Sletten, 2007). However, it is known that the NMR effect is not only dependent on the nuclei present in the molecular systems but also to the chemical environment around them. The NMR effect is sensitive to both the intra- and the intermolecular interactions in which a particular atom is engaged. Differences in the electronic environments cause the nucleus to experience slightly different applied magnetic fields owing to the shielding/deshielding effect of the induced electronic magnetic fields (Gil *et al.*, 1987). As a result, the same types of nucleus give rise to NMR signals at different spectral positions, which are determined by the effect of the surrounding electronic vicinity on the external magnetic field B_0. Moreover, most of the NMR signals do not appear as singular signals. In fact, due to spin-spin coupling that occurs between nonequivalent nucleus the NMR signals are frequently split in duplets, triplets, etc. Thus, considering ethanol as an example, the ^1H NMR spectrum has a profile presented in Figure 6. In this case, there are three types of protons: CH_3, CH_2 and OH. The CH_2 protons, which are closer to the oxygen atom and thus are less shielded, give rise

to a signal close to 1.0 ppm. As can be seen, this signal corresponds to a triplet of 1:2:1 relative intensities due to spin coupling with the directly linked CH_3 group. The methyl protons on the other hand give rise to a quartet of relative intensities 1:3:3:1 close to 3.5 ppm. This signal splitting results from the spin-spin coupling with the CH_2 protons. Finally, the third signal at around 4.7 ppm is related to the hydroxyl proton which is the most deshielded due to the direct linkage to the oxygen atom (Gil *et al.*, 1987; Nascimento and Bloch 2001; Claridge 1999).

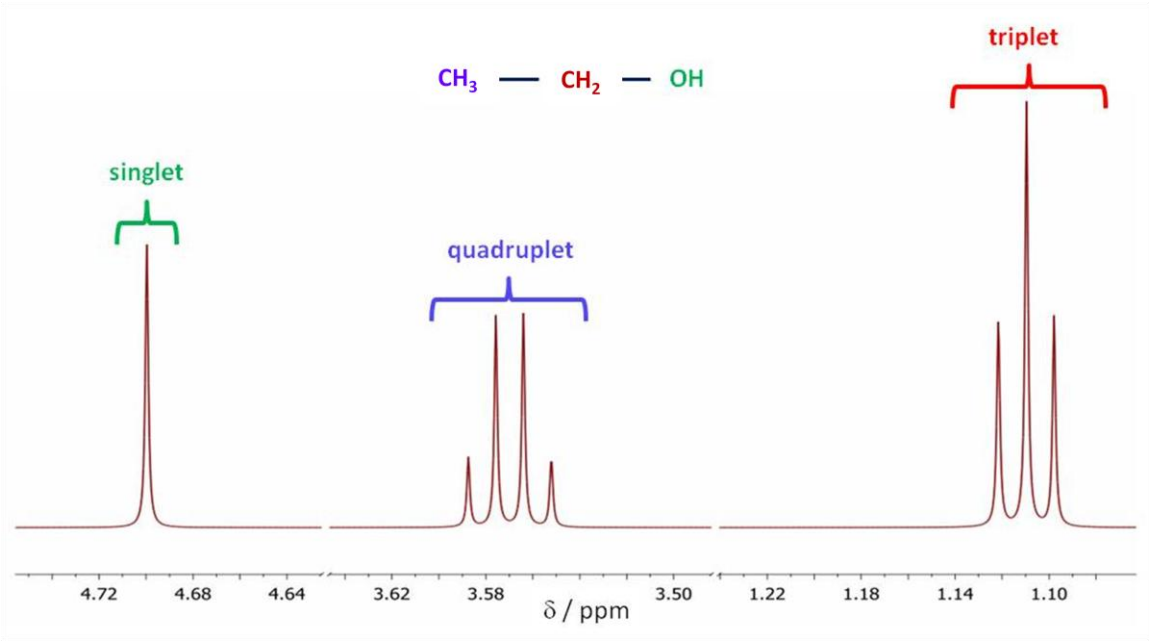

Figure 6: NMR spectrum of ethanol at 500 MHz (adapted from http://nmr-analysis.blogspot.com/2008/01/1h-nmr-analysis-common-myths-and.html)

The spectral information of solid and/or semi-solid samples, such as intact cells, is, however significantly limited due to the widening of the signals. This effect is due to three main factors, namely anisotropy of the chemical shifts, heterogeneity of magnetic susceptibility in the samples and dipolar coupling. All these effects may, however, be significantly attenuated. For instance, the signal widening due the dipolar coupling (D) is significantly reduced when the sample is disposed according to a specific angle θ in relation to B_0. Due to the observed proportionality between D and θ

$$D \propto \pm \mu_B r_{AB}^{-3} \left(3\cos^2\theta - 1\right)$$

where μ_B stands for magnetic momentum of nuclei B, r_{AB} is the internuclear distance between nuclei A and B and θ represents the angle between the internuclear vector and B_0. According to these relation, when θ takes a value of exactly 54.74º the term becomes null and, thus, the dipolar

coupling is cancelled. For this reason, this angle magnitude is designated as magic angle (Claridge, 1999; Sitter *et al*., 2009). The signal widening due to the anisotropy of the chemical shifts, on the other hand, is resolved by rotating the samples at high velocity during spectral recording. The minimal effective rotation velocity increases with the B_0 value. Finally, the effect of the differences in magnetic susceptibility within the sample may be minimized by milling finely the sample and by its spherical disposition within the sample holder in the probe.

Good attenuation of the signal widening is only achieved when both sample inclination and fast-velocity rotation are used simultaneously as represented schematically in Figure 7. In this case, the spectral resolution achieved is very similar to that observed for liquid sample NMR spectra. For this reason, the technique is known as High-Resolution Magic Angle Spinning (HR-MAS).

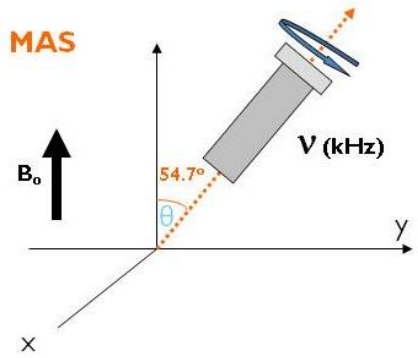

Figure 7: Esquematic representation of a sample rotating according to the magic angle

HRMAS has been successfully used for the metabolic profiling of different types of tissues, including normal and cancerous ones (Duarte *et al.*, 2009 a; Sitter *et al.*, 2008). In addition, HRMAS shows great potentials for the identification of biomarkers, an important step for detecting potential toxic effects of drugs as well as for early detection of diseases including cancer (Shanaiah *et al.*, 2008; Lindon *et al.*, 2004).

These improvements have expanded the NMR applicability hugely turning it to a central technique in drug discovery and design. It has been successfully used in the identification of lead and target structures, in the optimization of lead-target complexes as well as in the elucidation of reaction mechanisms (Vinje and Sletten, 2007; Cox *et al.*, 2006; Wider, 2002). In recent years, NMR spectroscopy has been increasingly employed for the analysis of metabolic processes occurring in biological systems (Duarte *et al.*, 2009 a; Merz and Serkova, 2009). This results from its ability to provide a rapid detection of several metabolites occurring in either biological systems, such as biofluids, cells and tissues. More recently, this spectroscopic technique has been employed

to study cancer and the effects of some drugs on these abnormal cells (Sitter *et al.*, 2009; Daly, 1988; Lindon *et al.*, 2004).

2.4.2 NMR techniques for the analysis of cultured cells

As stated previously, NMR spectroscopy provides detailed information on the molecular structure of systems as a function of its atomic constitution and intra- and inter-molecular interactions between components and solvent molecules. One clear advantage of NMR spectroscopy is the fact that it is a suitable tool for analyzing samples, pure or mixtures, either in liquid (namely, aqueous) or solid phases. Moreover, sample preparation requirements are usually minimum. When studies on cells and/or tissues are aimed, the sample preparation generally involve acidic (*eg.*, with 7-12% percholric acid) or dual-phase methanol-chloroform extractions, depending on the molecular systems attained followed by pellet redissolution in a deuterated solvent (Merz and Serkova, 2009).

The use of different NMR probes allows identifying distinct cellular metabolic biomarkers and following their concentration variation in the system. By this way, NMR experiments are a suitable tool to establish cause-effect relationships. For instance, it may allow to identify the cellular pathways that are affected by a particular drug and to follow its effect during continuous drug administration (treatment) (Tiziani *et al.*, 2009 b; Centerwall *et al.*, 2008). Similarly, the synergetic effect of two or more drugs may also be studied by using this spectroscopic technique. In the context of studying transformed cells (*eg.*, cancer cells), NMR spectroscopy opens a window for the identification and quantification of certain associated biomarkers, an important step in early detection of diseases (Tisiani *et al.*, 2009 a; Centerwall *et al.*, (2008); Tisiani *et al.*, 2009 b; Sellem *et al.*, 2011; Ludwig *et al.*, 2009; Khool and Al-Rubeai, 2007).

Other technique developments achieved in the last decades explain the importance of NMR spectroscopy in this research field. For instance, the use of two-dimensional (2D) NMR spectroscopy increases signal dispersion and yields lights on the connectivities between signals, thus helping in metabolite identification (Lindon and Nicholson, 2008). Moreover, the development of high-resolution magic angle spinning (HRMAS) spectroscopy increased the potentials of NMR spectroscopy for studying solid and semisolid (*eg.*, cells, tissues and organs) samples (Sitter *et al.*, 2009; Lião *et al.*, 2010; Sellem *et al.*, 2011). Using this technique, a significant resolution improvement is achieved even when aqueous- and lipid-soluble metabolites are observed *in situ* simultaneously (Griffin and Shockcor, 2004).

2.4.3 The metabonomics approach

In a simple definition, metabonomics or metabolomics is the study of the metabolic components of cells, tissues, organs or even organisms. The main goal is to identify and understand the cellular pathways that are perturbed as a consequence of a given pathology, treatment (therapy) or any other external stimuli. The concentrations of particular cellular metabolites may be regarded as sensitive markers of the genomic changes and responses of cells and tissues to external stimuli. In this way, the development of consistent tools for metabolomics studies greatly facilitates the understanding of the *in vitro* and *in vivo* actions of the available drugs as well as aid in the setting of new more effective therapies (Tiziani *et al.*,2009 b; Lindon *et al*., 2004). NMR spectroscopy is one of the main analytical techniques used to obtain the data to be used in metabolomics studies (Lindon and Nicholson, 2008; Wishart, 2008; Merz and Serkova, 2009; Griffin and Shockcor, 2004).

The basic workflow of NMR-based metabolic analysis is as follows: sample preparation (which may involve quenching/extraction of metabolites) → data collection → data processing → data analysis, employing multivariate statistics to deal with the complexity of the spectral information collected. The success and applicability of this approach is strongly dependent on the data processing step, which includes spectral normalization and baseline correction. This step ensures for strict sample uniformity to reduce statistical problems from improper baseline distortion, line-width differences or natural chemical-shift draft (Wishart, 2008).

The data analysis step that involves the interpretation of the NMR signals is not always an easy task, particularly when complex mixtures as those present in cell or tissue samples are under study. In other words, the data point intensities in an NMR spectrum is a multidimensional graph of metabolic coordinates. Then, the initial objective in metabonomics is to classify a particular sample on the basis of its identified spectral patterns and subsequently identify the metabolic features underlying its classification. In order to give scientific consistency and support to the interpretations done, considerable efforts are being performed for the last decades into the development of algorithms capable to align the signals ascribed to the same but observed in data acquired for different sample mixtures. In other words, there is a continuous search for multivariate statistical analysis methods capable of reducing the data space dimension in an efficient and accurate way (Lindon and Nicholson, 2008).

In this context, one of the unsupervised methods extensively used in NMR-based metabonomics studies is the principal components analysis (PCA) technique (Lindon and Nicholson, 2008). Within PCA, the multidimensional data matrix is converted to principal components, yielding two matrices known as scores and loadings. The scores are linear combinations of the original variables while each principal component (PC) loading defines the way the old variables are linearly combined to form the new variables. Thus, each point in a score

plot represents a spectrum of one single sample, while in a loading plot each point represents a distinct spectral intensity. By observing both plots it is possible to interpret the spectral clustering observed in a score plot based on the corresponding loadings that cause cluster separation (Lindon and Nicholson, 2008).

Besides unsupervised methods like PCA, several supervised methods (that use a training set of data with known endpoints) have also been developed. Among them, one of the most widely used is the partial least squares (PLS) method. Within this multivariate statistical methodology, a data matrix containing independent variables related to different samples (*eg.*, spectral intensity values) is related to another matrix containing dependent variables (such as values related to the response measurements) of the same samples. Coupling PLS to discriminant analysis (DA) allows establishing the optimal position to place the discriminant surface that best separates the classes (Lindon and Nicholson, 2008).

In the present work, the two types of multivariate statistical analysis (PCA and PLS-DA) have been employed to identify and correlate the spectral changes promoted in the ^{1}H HRMAS NMR spectra of the lung cancer cell line A549 by exposure to either CDDP or 6 Gy ionizing radiation. Hopefully, this will give some contributions for the understanding of the cellular behavior, namely metabolic pathway changes, promoted by those chemical and physical effects (drug and radiations exposures).

2.4.4 NMR studies of cancer cells and their responses to antitumoral agents

One research area in which the method has been successfully used is the monitoring of tumor growth and regression (Jansen *et al.*, 2002; Stenman *et al.*, 2011). This clearly opens the door for the identification and understanding of the pathogenic mechanisms underlying cancer evolution as well as to follow the effect of particular therapies. As easily understandable, this is also of particular relevance in the field of the design of new more effective anticancer drugs and/or therapy protocols as a function of biochemical targets (Lindon and Nicholson, 2008; Bayet-Robert *et al.*, 2010). In a recent work, Bayet-Robert *et al.*, evaluated the cytotoxicity of several marine natural products (MNPs) in breast cancer MCF7 cell line. The ^{1}H HRMAS NMR spectroscopy-based metabolomic investigation performed allowed establishing the potential targets of the MNPs as well as the mechanisms underlying the cellular response. For instance, it was found that the marine topoisomerase II inhibitor ASC blocks the enzyme of the tricarboxilic acid cycle (TCA) while Lam-D, a pyrrole alkaloid, induces disorders at the mitochondrial-cytosolic carrier systems. The results also showed the cyclic depsipeptide KF enhances the catabolism of membrane lipids (Bayet-Robert *et al.*, 2010).

^{1}H NMR spectroscopy has also been used to define the metabolic phenotypes of tumor cells. Griffin *et al*., determined the inherent and specific metabolic profiles characterizing the major brain tumor cell types (Griffin and Kauppinen, 2007). In addition, HRMAS NMR spectroscopy was used by Sellem *et al.*, to discriminate between healthy and carcinoma ovarian epithelial tissues (Sellem *et al.*, 2011). The results showed that the most common feature in all ovarian carcinomas is the enhanced level of total choline-containing compounds, in similarity to what was reported by others for different types of tumors (Duarte *et al.*, 2009 b; Sitter *et al.*, 2009; Merz and Serkova, 2009; Jansen *et al.*, 2002; Zira *et al*., 2010; Griffin and Kauppinen, 2007). Moreover, Sellem *et al.*, showed that the type of choline-containing compound which level is increased depends on the type of ovarian carcinoma (Sellem *et al.*, 2011).

Many other recent applications of HRMAS NMR spectroscopy based metabolomics in the field of oncology are found in literature, and have been compiled in several published reviews (Sitter *et al.*, 2009; Merz and Serkova, 2009; Griffin and Shockcor, 2004). All together, those studies allowed establishing some of the main metabolic markers characterizing different cancer types, thus contributing to an understanding of the biochemical mechanisms underlying their content level in the cell (Table 2). On the whole, the combined used of different metabolomic NMR measurements (for instance, using different NMR probes) can allow the profiling of about 1000-2000 metabolites (Cuperlovic-Culf *et al.*, 2010). Although this does not cover all the metabolites present in a complex biological system as a cell, it provides a large pool of information and a good cover of most of the metabolic processes occurring in a cell, which are highly correlated to each other (Cuperlovic-Culf *et al.*, 2010).

The identification of the main biomarkers characterizing a particular cancer type opens the doors for the understanding of the cellular responses to a particular drug or combination of drugs applied (Merz and Serkova, 2009). Tiziani *et al.*, for instance, showed that acute myeloid leukaemia cells are sensitive to the combined administration of Bezafibrate (BEZ), a lipid lowering drug, and Medroxyprogestrone acetate (MPA), a contraceptive steroid. The response to treatment has been correlated to the downstream effect of ROS (reactive oxygen species) on the TCA cycle (Tiziani *et al.*, 2009 b). The PCA analysis performed by the authors clearly showed that the K562 and KG1a cell lines have a similar metabolic response to the BEZ+MPA treatment, while the HL-60 line responded in a completely different way. The observation of the NMR signals related to small and mobile molecular species have been considered as a valuable tool for the early detection of cellular apoptosis induced by chemotherapeutic cytotoxic drugs (Tiziani *et al.*, 2009 b; Bezabeh *et al.*, 2001; Duarte *et al.*, 2010). More recently, ^{1}H NMR was used to monitor the hydrolytic degradation of micelles developed for the delivery of the anticancer drug doxorubicin (Chen *et al.*, 2011). All this, shows that NMR spectroscopic studies may significantly contribute not just for the

routine structural characterization of drugs, but also to the understanding and bettering of the processes involved in drug´s anticancer activity and delivery.

Table 2: Main metabolic biomarkers of tumours (adaptated from Griffin and Kauppinen 2007; Griffin and Shockcor, 2004; Merz and Serkova, 2009)

Metabolite	Metabolic function
Alanine	Increases in hypoxic tissues as a result of increased glycolysis
ATP	Decreased ATP production due to glycolytic phenotype; increased ATP utilization due to fast cell proliferation rate
CH_3 & CH_2 lipids	Increases in the relative intensities of lipid peaks detected by NMR are believed to result from either the production of cell membrabe microdomains or increased numbers of cytoplasmic vesicles
Choline containing metabolites (CCMs)	Choline, phosphocholine, phosphatidylcholine and glycerophosphocholine are major constituents of cell membranes and increases in these metabolites reflect cell death (apoptosis and necrosis)
Citrate	Decreased in prostate tumors due to disturbances in Zn metabolism
Glycerophosphocholine	Catabolic product of membrane phospholipids; decreased due to downregulated apoptosis
Glycine	An amino acid and an essential precursor for *de novo* purine formation
Lactate	Lactate is an end product of glycolysis and increases rapidly during hypoxia and ischaemia, in particular as a result of poor vascularity and acquired resistance to hypoxia
Myo-inositol	In tumours, myo-inositol is involved in osmoregulation and volume regulation
Nucleotides	Used to manufacture DNA and RNA; also key metabolic intermediates in fatty-acid and glycogen metabolism; changes in ATP concentration also indicate the energetic status of the tumour
Phosphocholine	Precursor for membrane phospholipids ; enzyme induction owing to high proliferation rate
Taurine	Important in osmoregulation and volume regulation; hypotaurine is also an antioxidant and might protect cells from free-radical damage

Cisplatin (cis-diamminedichloroplatin (II); CDDP; Figure 8, a neutral platinum (II) complex with planar square structure, was firstly synthesized by Peyrone in 1845 and its molecular structure was determined by Alfred Werner in 1893 .However, its anticancer activity was only discovered accidentally by Rosenberg in the 60th, while its approval by the Food and Drug Administration (FDA) for clinical use dates from 1978 (Siddik, 2003).

CDDP is still among the most widely used drugs in cancer chemotherapy. It displays significant activity against several types of neoplastic disorders, with special success against head, neck, testicular and ovarian cancers (Carloni and Alber, 2003). Still not fully understand is the fact that its *trans* isomer (transplatin, trans-diamminedichloroplatin (II); tDDP) is found to be totally inactive from the chemotherapeutic point of view.

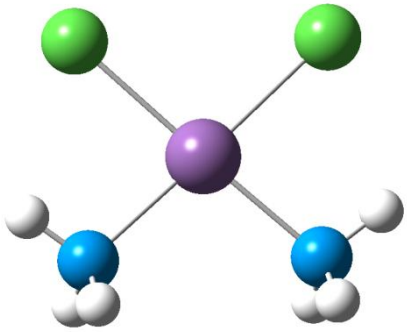

Figure 8: Molecular structure of CDDP (drawn using the GaussView software)

The most likely target of CDDP, correlating with anti-tumor activity, has been shown by many works to be the cellular DNA. Several distinct adducts can be formed by CDDP binding to DNA (Figure 9) (Carloni and Alber, 2003). The most important are the intrastrand adjacent 5´-GG bi-adducts that account for about 65%, followed by the 5´-AG bi-adducts that account for 25 %. Less frequent, but still accounting with more than 5%, are the nonadjacent intrastrand didentate adducts GXG, where X stands for any other nitrogenated DNA base (6%). Other types of CDDP-DNA adducts comprise monofunctional drug binding to one guanine residue and interstrand bifunctional GG ones. The formation of these adducts induce distortions of the tertiary structure of DNA that depend on the type of adduct formed. The 5´-GG bi-adduct, for instance, has been determined to disrupt the helical structure of DNA be de-stacking the two adjacent base pairs and locally unwinding the molecule at the site of the lesion. This creates a hydrophobic pocket facing the minor groove that is widened and flattened. As a consequence, the replication and transcription machinery of the cell is inhibited (Carloni and Alber, 2003).

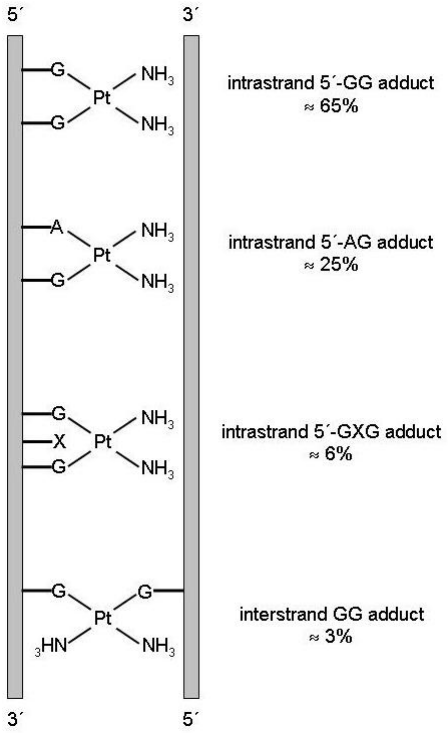

Figure 9: Schematic representation of the different DNA adducts formed by CDDP (adapted from Carloni and Alber, 2003)

However, the mechanism of action of CDDP involves several steps prior to its binding to the DNA molecule (Figure 10). Cisplatin is given to the patients by injection. Outside the cells, the high concentration of Cl^- ions (higher than 100 mM) prevents chloride hydrolysis. However, after entering the cell through either passive diffusion or by active transport (by transmembrane transporters, as the copper transporter CTR1, CDDP deals with much lower chloride concentrations (below 20 mM), being the drug activated by hydrolysis and/or reaction with other ligands, particularly those containing sulfur donor groups (as proteins, aminoacids and glutathione) (Wang *et al.*, 2011).

Only a part of the activated platinated species (either aqua- or sulfur-containing species) reaches to enter the nucleus and subsequently reacts with DNA. The resultant kink and unwinding of the DNA molecule is recognized by specific cellular proteins. This may result in either DNA repair, by cutting out the Pt-containing fragment followed by resynthesizing of the open sites, or in no DNA repair, followed by apoptosis and cell killing. The remaining platinum not entering the nucleus seems to be excreted by the cell through different manners, one involving the copper transporters ATP7A and ATP7B (Reedijk, 2009).

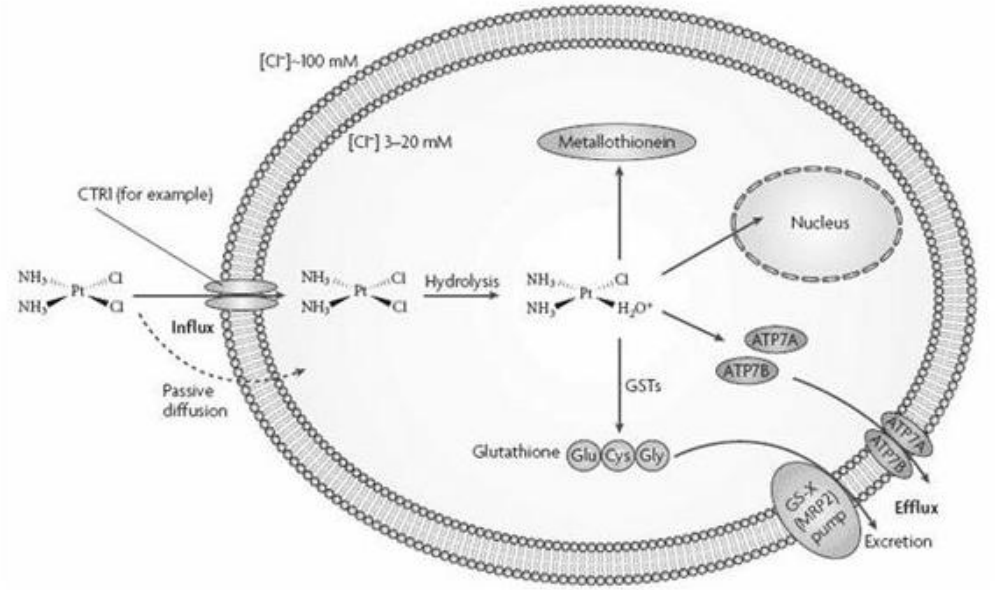

Figure 10: Schematic representation of the molecular mechanisms underlying CDDP cell entrance, activation and adducts formation (taken from Medscape.com)

Being the hydrolysis reaction a key step in CDDP activation, it does not surprise that many NMR studies have been devoted to the speciation of the CDDP aqueous solution and to the determination of the kinetic parameters underlying drug activation (hydrolysis) (Vinje and Sletten, 2007; Berners-Prince *et al.,* 2006; Davies *et al.,* 2000 a). The interaction of the CDDP hydrolytes with different cellular metabolites, namely sulfur-containing aminoacids, proteins and glutathione, have also been extensively analyzed by means of NMR spectroscopic techniques using different probes (Berners-Prince *et al.,* 2006; El-Khateeb *et al.,* 1999). Wang *et al.,* used 2D NMR to probe the binding site of CDDP to human copper transporter (hCTR1), a step believed to be important in the influx of the drug. The interaction of CDDP and its hydrolytes with DNA has also deserved special attention in the field of NMR techniques (Reeder *et al.,* 1997; Davies *et al.,* 2000 b; Davies *et al.,* 2000 a; Davies *et al.,* 1998; Wang *et al.,* 2011).

In what concerns the study of the effect of CDDP on intact cells by means of NMR spectroscopy, two studies deserve special reference in the present study. One of those studies focused on relationship between the changes promoted by CDDP exposure on the membrane lipids of the herein studied cell line (A549) and the development of drug resistance by these cells (Huang *et al.,* 2003). The study clearly showed that exposure to CDDP promoted significant changes in the membrane lipids of both sensitive and resistant A549 cell lines. However, the spectral evidences also indicated that the differences are significantly different in the two cell lines. In a more recent study (Duarte *et al.,* 2010) the effect of CDDP exposure of MG-63 osteosarcoma cells has also

been analyzed by ^{1}H NMR spectroscopy. The coupling with multivariate studies allowed profiling the metabolic changes promoted by the drug over time of exposure. Both studies constitute a good starting point for the herein reported study.

2.4.5 **NMR studies of cellular responses to radiation**

Exposure of cells to ionizing radiation leads to cellular damages, primarily through a spectrum of DNA lesions, among which the break of the double-strand represents the most lethal form of damage (Marekova *et al.*, 2003; Tucker, 2008; Santini *et al.*, 2006). The produced lesions are recognized by a number of proteins (*eg.*, DNA-dependent protein-kinase), which are activated leading to a signal transmission to other proteins (*eg.*, p53) which are also activated. p53-protein is a tumor suppressor gene product, whose function is to induce DNA repair, cell cycle arrest and apoptosis (Marekova *et al.*, 2003; Suzuki *et al.*, 2001; Luciani *et al.*, 2009). Besides the damages caused at the DNA level other pathways have been referred as being changed by ionizing radiation. For instance, exposure to ionizing radiation has been correlated with processes of lipid peroxidation and protein oxidation, in membranes, cytoplasm and nucleus (Suzuki *et al.*, 2001; Durovic *et al.*, 2004; Puthran *et al.*, 2009). Moreover, it has been reported that the exposure to radiation, as chemotherapeutic drugs, leads to an increase of ceramide concentration, a pathway that seems to be initialized by changes in cell membranes (Marekova *et al.*, 2003).

In the last years, several reports refer that low-dose ionizing radiation enhances cell proliferation (Kim *et al.*, 2007; Suzuki *et al.*, 2001; Parthymou *et al.*, 2004; Liang *et al.*, 2011). Using normal human lung fibroblasts exposed to a 0.05 Gy ionizing radiation, Kim *et al.*, concluded that cell proliferation was enhanced through activation of ERK1/2 and p38 genes (Kim *et al.*, 2007). A similar conclusion was also reported by Suzuki *et al.*, who exposed normal human diploid cell HE49 to radiation doses between 1 cGy and 6 Gy (Suzuki *et al.*, 2001). According to the authors, doses between 2 and 5 cGy stimulate cell proliferation while doses greater than 1 Gy show lethal effect on cells. Parthymou *et al.*, showed that the decrease of the number of C6 glioma cells 48 h after irradiation is only evident at doses greater than 5 Gy. A prior work on GH3 cells (from rat pituitary adenoma) showed that the metabolic viability of the cells is significantly affected upon exposure to ionizing radiation, being the effect time- and dose-dependent. The degree of the proliferation rate inhibition increased with the ionizing radiation dose, with the survival rate being of just 0.46% for a dose of 6 Gy (Parthymou *et al.*, 2004).

In this context, NMR spectroscopy, particularly using the ^{1}H probe, contributed significantly for the understanding of the main metabolic pathways being affected by the exposure to ionizing radiation. In general, these reports refer that cell radiation leads to an increase of the NMR

resonance lines related to the methyl groups, especially CH_2, of fatty acid acyl chains (Matulewicz *et al.*, 2006; Santini *et al.*, 2006; Santini *et al.*, 2006 a; Mahmood *et al.*, 1994; Merz and Serkova, 2009). As in result of other external estimuli, this effect has been related to an increase of CH_2 and CH_3 mobile lipids in consequence of cell death due to membrane damaging (Matulewicz *et al.*, 2006; Hendrich, 2003).

Luciani *et al*., compared the behavior with respect to the variation of the methyl signals of mobile lipids, in two distinct cell lines (MCF-7 and HeLa), kept in culture with and without prior irradiation. According to the results, the CH_2 and CH_3 signals of the cells cultured without prior irradiation showed an initial intensity decrease that was followed by a subsequent recovery. When using irradiated cells, the effect on these signals showed a cell type-dependency. For the MCF-7 cell line, the recovery of the mobile lipids signals was significantly faster with respect to the non-irradiated counterparts, while for the HeLa cells the opposite was the case. According to the authors, this distinction is probably associated to the fact that the HeLa cells in contrast to the MCF-7 ones do not present functional p53 protein (Luciani *et al.*, 2009).

Besides the variations observed for the mobile lipids content, other metabolites were found to be affected by the irradiation procedure (Mahmood *et al.*, 1994; Santini *et al.*, 2006; Santini *et al.*, 2006 a; Merz and Serkova, 2009). For instance, Santini *et al.*, refer an increase of the GSH level in MG-63 osteosarcoma spheroids irradiated with a 5 Gy ionizing radiation following a prior decrease in the first 24 h (Santini *et al.*, 2006; Santini *et al.*, 2006 a). Accomplishing the GSH increase observed 48 h after irradiation, the authors also observed an initial decrease of the glutamine and glutamate levels relative to the control, but stabilization of the content of these metabolites is observed for after 72 h. It should be recalled that glutamine and glutamate are percursor/intermediate in the GSH biosynthesis pathway (Figure 11). An explanation of the effects observed by Santini *et al*., is easy of this metabolite interaction is taken into account. When the cells are subjected to an ionizing radiation, this causes oxidative stress, and by this way irradiation leads to a decrease of the GSH level due to its conversion to the oxidized form. To keep GSH production at levels that ensure the survival of the cells (after the initial 24 h) it becomes necessary to recover the GSH level what leads to a decrease of the precursors glutamine and glutamate. After some time, the cell has to increase also the biosynthesis of those precursors in order to keep the GSH pathway active (Santini *et al.*, 2006 a).

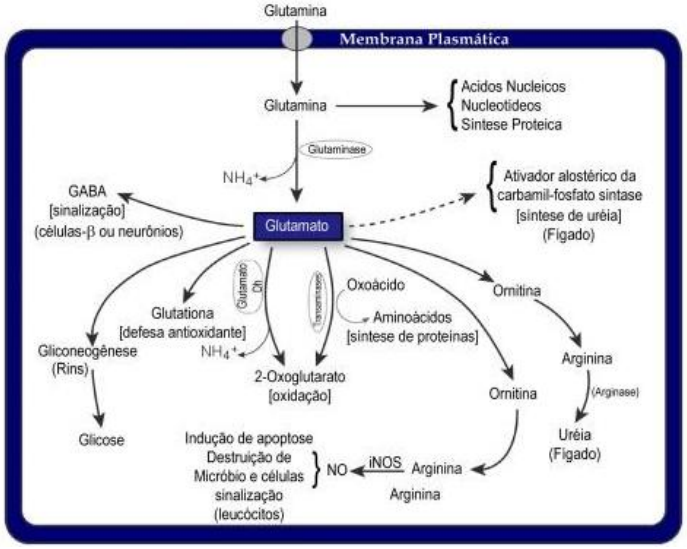

Figure 11: Pathways of glutamine metabolism (taken from http://www.proximus.com.br/news/content/suplementacao_com_l_glutamina_e_desempenho_fisico)

Finally, using ^{31}P NMR probe allowed following the variations of the level of other metabolites containing this nucleous. Several studies report the decrease of the content in choline-containing metabolites, including phosphocholine (Santini *et al.*, 2006; Santini *et al.*, 2006 a; Merz and Serkova, 2009; Mahmood *et al.*, 1994). These results point to an effect of radiation on the phosphatidylcholine metabolism, one of the main constituent of cellular membranes and is in line with the NMR results obtained by other investigators on other cell lines in which apoptosis is promoted with other external stimuli (Santini *et al.*, 2006 a; Hendrich 2003).

Many other metabolite level variations in irradiated cells were followed by NMR spectroscopy as a function of recovery time and cell type. All together they prove the usefulness of this spectroscopic technique for identifying and quantifying the effects of radiation in biological systems, and open a door for the understanding of the mechanisms of cancer promoting factors as well as for the development of fast and early detection of cancer formation (Santini *et al.*, 2006; Santini *et al.*, 2006 a; Merz and Serkova, 2009).

Materials and Methods

3. Materials and Methods

3.1 Culture of human lung cells from tissue biopsies

Lung carcinomas fresh tissues were obtained from surgical specimens following the local ethic committee rules. Immediately after surgery, Pathologists included exceeding tumoral tissues (8mm^3) in a Hank´s solution (Gibco) to be transported to the research laboratory.

Tumor fragments were minced into very small pieces with scalpels. The small pieces were seeded with a pipette into 25 cm^2 flask and a drop of serum free medium was added being the excess removed. The DMEM/F-12 (Gibco) medium, supplemented with 5% fetal bovine serum (FBS) (Gibco), 30 nM sodium selenite (Sigma), 10 μM ethanolamine (Sigma), 10 μM phosphorylethanolamine (Sigma), 0,5 μM sodium pyruvate (Gibco), 2 mM glutamine (Gibco), 5 μg/ml insulin (Sigma), 5 μg/ml transferring (Sigma), 10 ng/ml EGF (Sigma), 100 nM hydrocortisone (Sigma), and antibiotics (penicillin-streptomycin) (Gibco), was used. The flaskes were at 37º C in a humidified atmosphere under 5% CO_2. Seven days after seeding, the cells were observed under the microscope and the medium was replaced. When confluence was observed, the cells were harvested by addition of trypsin (0,05% trypsin/EDTA solution) (Gibco) and plated into new flasks. All cultures were cryopreserved for further studies.

The established cultures were evaluated by immunocytochemistry, in order to verify phenotypes after cell seeding on glass slides to characterize cell morphology developed in the culture flasks. As the cells grow in monolayer, they were trypsinized at 37º C and transferred to glass slides, which were subsequently placed in 95% alcohol (Merck). The immunocytochemical studies were carried out at the Institute of Pathology of the Faculty of Medicine of the University of Coimbra.

The above described procedure was completely repeated and accomplished on macroscopically normal pulmonary tissue, as Pathologists followed the same protocol in exceeding peri-tumoral tissue.

In Table 3, the studied bronchial-pulmonary carcinomas are listed recording histological classification, morphological patterns and staging.

Table 3: Histological Classification and Staging of Bronchial-Pulmonary Carcinomas

Cell lines	Histological typing	Staging
PP1	Adenocarcinoma mixed type (acinar & solid)	pT2bN0Mx
PT1		
PP2	Adenocarcinoma mixed type (BA & acinar & micropapillary & Solid)	pT2aN0Mx
PT2		
PP3	Adenocarcinoma mixed type (BA & micropapillary & Solid)	pT2bN1Mx
PT3		
PP4	Adenocarcinoma mixed type (papillary & acinar)	pT2bN0Mx
PT4		
PP5	Lymphoepithelial carcinoma	pT1bNxMx
PT5		
PP6	Pleomorphic Carcinoma (acinar & papillary & large cell)	pT2bN0Mx
PT6		
PP7	Acinar adenocarcinoma	pT1bN0Mx
PT7		
PP8	Acinar adenocarcinoma	pT1bN0Mx
PT8		
PP9	Adenocarcinoma mixed type (acinar & solid)	pT2bN0Mx
PT9		
PP10	Squamous cell carcinoma	pT2aN0Mx
PT10		
PP11	Pleomorphic carcinoma (ADSQ & large cell & NE)	pT1aN0Mx
PT11		
PP12	Adenocarcinoma mixed type (acinar & solid with mucus)	pT2bN0Mx
PT12		
PP13	Squamous cell carcinoma	pT2aN0Mx
PT13		
PP14	Squamous cell carcinoma	pT2bN0Mx
PT14		
PP15	Adenocarcinoma mixed type (acinar & papillary)	pT2aN2Mx
PT15		
PP16	Squamous cell carcinoma	pT2aN1Mx
PT16		
PP17	Squamous cell carcinoma	pT2aN0Mx
PT17		
PP18	Adenocarcinoma mixed (micropapillary & MUC 2+)	pT2bN1Mx
PT18		
PP19	Squamous cell carcinoma	pT1aN0Mx
PT19		
PP20	Adenocarcinoma mixed (acinar & papillary & micropapilly)	pT3N0Mx
PT20		
PP21	Pleomorphic carcinoma (fusiform & LC & GC)	pT1aN0Mx
PT21		
PP22	Pleomorphic carcinoma (BA & GC)	pT2aN0Mx
PT22		

PT- Pulmonary Tumor and PP- Pulmonary Parenchime; BA – Brochial alveolar (lepidic); ADSQ – Adenosquamus arcinoma; NE – Neuroendocrine; LG – Large cell and GC – Giant cell

3.2 Immunohistochemistry

The immunohistochemical studies were then performed on glass slides with cells of the cultures obtained from tumoral and lung tissue samples. After fixation in ethanol at 95%, the samples were rehydrated. The endogenous peroxidase activity was quenched by incubation in 3% diluted hydrogen peroxide (H_2O_2) during 15 minutes. For blocking nonspecific binding with primary antibodies we used Ultra V Block (Ultra Vision Kit; TP-125-UB; Lab Vision Corporation; Fremont CA; USA).

Different primary antibodies were considered to distinguish epithelial characteristics. Cytokeratin 5/6/18 (clone LP34, Novocastra Laboratories Ltd, Newcastle, United Kingdom) was applied to characterize Squamous Cell Carcinoma, at a dilution of 1:100 for 60 minutes; CK7 (clone OV-TL 12/30, DakoCytomation, Glostrup, Denmark), at a dilution of 1:50 for 30 minutes and TTF1 (clone 8G7G3/1, DakoCytomation, Glostrup, Denmark), at a dilution of 1:100 for 60 minutes were chosen to identify adenocarcinomas cells. All slides incubations were performed at room temperature. After incubation with the antibodies, the slides were washed with phosphate-buffered saline (PBS) (Ultra Vision; TP-125- PB; Lab Vision Corporation; Fremont CA; USA) and subsequently incubated for 15 minutes with biotin-labeled secondary antibody (Ultra Vision Kit; TP-125-BN; Lab Vision Corporation; Fremont CA; USA). The primary antibodies' binding was localized in cells using peroxidase-conjugated streptavidin (Ultra Vision Kit; TP-125-HR; Lab Vision Corporation; Fremont CA; USA). According to the manufacturer's instructions, 3,3-diaminobenzidine tetrahydrochloride (DAB) (RE7190-K; Novocastra Laboratories Ltd, Newcastle, United Kingdom) was used as chromogen. In addition, haematoxylin passing followed to counterstain the slides before dehydration and mounting. In parallel, known positive and negative controls were also stained.

3.3 Studies with the lung cell line A549

3.3.1 Cell Culture

Lung cancer cell line A549, kindly provided by the Laboratorio de Biologia Molecular Aplicada Faculdade de Medicina da Universidade de Coimbra, were grown in Dulbecco's Modified Eagle Medium (DMEM) (Gibco) supplemented with 10% fetal bovine serum (Gibco), 2 mM glutamine (Gibco) and antibiotics (penicillin-streptomycin) (Gibco), and maintained at 37º C in a humidified atmosphere under 5% CO_2.

3.3.2 Cytogenetic analysis

To check the type of chromosomal alterations occurring in the cell line A549, karyotyping studies were performed. For that, 100 μl of Colcemid (Gibco) was added to the cells in order to inhibit the mitotic spindle (enabling the arrest of cell division in metaphase), and incubated for 3 hours. After this period, the number of dividing cells was determined by inverted microscope. The cells were then submitted to trypsinization and put in a 10 ml Falcon tube. The supernatant was removed and samples were submitted to centrifugation at 1000 r.p.m. for 6 minutes. The obtained pellet was ressuspended with 1 ml of FBS (Gibco), to protect the cells from bursting due to hypotonic shock, and 9 ml of KCL (Merck). The tubes were incubated at 37° C, with an inclination of 45º for 20 minutes. After this time, pre-fixation of the cells was performed with 120 μl of fixative agent 1:6 (methanol (Merck) / acetic acid (Merck)) and recovered by centrifugation at 1000 r.p.m. for 6 minutes. Finally, three successive fixations, using 4 ml fixative agents 1:6, 1:3 and 1:1, were made.

The manipulated cells were spread on glass slides, which were kept in a hothouse at 70º C (to make the chromosomes resistant to treatment with trypsin (Gibco), which is done during the GTG banding) about 3 hours. After this period they were stained. The slides were placed in trypsin for a few seconds, being the trypsin after that period inhibited with 5% FBS (Gibco). The slides were washed with a pH 6,8 buffer (Merck Microscopy), to remove the excess of trypsin. The chromosomes were stained in 10% Giemsa (Merck) and the excess removed with the prior buffer. The metaphases were analyzed by light microscope coupled to a computer system (Cytovision), where the images were saved for analysis.

3.3.3 Growth behaviour of the A549 cells and choice of CDDP concentration

Prior to the studies on the cellular responses to either CDDP or radiation exposure some parallel studies were performed in view of determining the optimal initial cellular density and the best CDDP concentration to be used. In what concerns the establishment of the growth curves used to determine the initial cellular density to be used the Trypan Blue method, which marks the cells presenting integral cellular membranes, was used. On the other hand, for determining the CDDP concentration to be used, the MTT test (3-4,5-dimethylthiazol-2-yl) 2,5-diphenyl tetrazolium bromide) (Sigma) was used for quantification of cell viability. According to the results obtained the best cellular density encountered for the studies is of 5.0×10^4 cell/cm^2. Moreover, the CDDP concentration chosen corresponds to a drug concentration of 50 μM that was found to lead to 50% cell death (IC50).

3.3.4 Exposure to cisplatin

Twenty-four hours after seeding, the cells were harvested by addition of trypsin (0,05% trypsin) (Gibco), plated in flasks (5.0 x 10^4 cell/cm^2, corresponding to 5x10^6 cells per flask) and maintained at 37º C in a humidified atmosphere under 5% CO_2. After other 24 hours, the experiment was initiated (t = 0) by adding to the flasks culture medium 50 μM CDDP (Sigma). In parallel an equally prepared an equal flask with no CDDP was maintained at the same conditions for control. At different time intervals (t = 0, 12, 18, 24, 36 and 48h), the adherent cells were harvested by trypsinisation, washed with phosphate buffer solution (PBS, pH 7,4) (Euroclone) and centrifuged at 1000 r.p.m. for 6 minutes. Lysed suspensions were then prepared as will be described below. Three independent assays (in duplicates) of each condition (time) were performed. For NMR analysis, the duplicates were mixed, to provide samples with a sufficiently large number of cells, in order to obtain good signal-to-noise spectra.

3.3.5 Exposure to radiation

Twenty-four hours after seeding, the cells were harvested upon addition of trypsin (0,05% trypsin) (Gibco), plated in flasks (5.0 x 10^4 cell/cm^2, corresponding to 5x10^6 cells per flask), and maintained at 37º C in a humidified atmosphere under 5% CO_2. After waiting more 24 hours for cells to adhere, the experiment was initiated (t = 0) by radiating flasks with a 6 Gy ionizing radiation. This radiation dose was chosen as it corresponds to the suboptimal dose delivered in radiotherapeutic protocols for human tumors and is known to induce damages in many cancer cell lines (Cataldi *et al.*, 2009).

Control cells were not submitted to radiation. At different time points (t = 2, 24, 48 and 72h), the adherent cells were harvested by trypsinisation, washed with phosphate buffer solution (PBS, pH 7,4) (Euroclone) and centrifuged at 1000 r.p.m. for 6 minutes. Lysed suspensions were then prepared as described below. Three independent assays (in duplicate) of each condition (time point) were performed. For NMR analysis, the duplicates were mixed, when necessary, to provide samples with a sufficiently large number of cells for good signal-to-noise spectra to be obtained.

3.3.6 Trypan blue Exclusion Assay

At each time point, the extent of cell death was assessed using the Trypan blue exclusion assay (Sigma). These dye exclusion test was used to determine the number of viable cells present in a cell suspension measure of cell membrane integrity. Briefly, cells were incubated with Trypan blue dye (0,4% (w/v) solution in PBS) and counted in a Neubauer-counting

chamber. Cell viability was expressed as the percentage of living cells (dye-excluding) relative to the total number of cells (mean ± SEM, standard error of the mean).

3.3.7 Cell sampling and preparation for NMR

The protocol used for preparing the cell samples for NMR analysis was chosen based on a previous study that tested the effects of different sampling and storage procedures on the cells integrity and metabolic profiles (Duarte *et al.*, 2009 b). In that study, mechanical cell lysis, although requiring special care in terms of reproducibility, was found to enable well-resolved spectra with good visibility of intracellular metabolites to be obtained by ^{1}H HRMAS, thus being the method of choice in the present work. Briefly, the cells were firstly washed with a PBS solution and then suspended in 1ml PBS/D_2O (0,14 M NaCl, 0,0027 M KCl, 0,0015 M KH_2PO_4, 0,0081 M Na_2HPO_4 in deuterated water, pH7,4), centrifuged and ressuspended in 40 µl PBS/D_2O, to which 5µl PBS/D_2O containing TSP 0,25% (for chemical shift referencing) were added. Then, a 3-fold cycle of liquid nitrogen deeping and sonication was performed to obtain a suspension of lysed cells. Each sample was then transferred to a NMR disposable insert with sealing cap and stored at -80º C until analysis.

3.3.8 NMR Measurements

The disposable inserts containing the cell samples were placed in standard 4 mm MAS rotors and analyzed in a Bruker Avance Spectrometer operating at 500 MHz for ^{1}H observation, using a 4 mm HRMAS probe, in which the rotor containing the sample was spun at the magic angle and a 4 kHz spinning rate. A standard 1D spectrum (pulse program "noesypr1d", Bruker library) was acquired for each sample with a spectral width of 6510 Hz, 32K data points, a 4 s relaxation delay and 256 scans.

All 1D spectra were processed with a line broadening and baseline corrected. The chemical shifts were referenced internally to the alanine signal at 1.48 ppm (this peak was found to be more reliable than the TSP peak due to the sensitivity of the latter to intermolecular interactions).

Finally, in order to facilitate spectral assignments 2D spectra were also recorded using the same acquisition conditions used in the 1D experiments.

3.3.9 Multivariate analysis of NMR spectra data

In the case of the experiments with CDDP-exposed cells, a total of 37 spectra were considered for the multivariate analysis, corresponding to 23 control sample and 14 treated

samples. In the case of the radiation experiments a total of 16 spectra were considered, corresponding to 8 control samples and 8 irradiated samples. Data matrices were built from standard 1D spectra (δ 0,25-10), and normalization was applied by adjusting the total area to unity. Then, after appropriate scaling (unit variance), Principal Component Analysis (PCA) and Partial Least Squares Regression Discriminant Analysis (PLS-DA) were applied to the data using Simca-P 11,5 (Umetrics, Sweden), employing a default 7-fold internal cross validation, from which Q^2 and R^2 values, representing, respectively, the predictive capability and the explained variance, were extracted.

Results and discussion

4 Results and discussion

4.1 Tentative establishment of primary lung cell cultures

Cultured primary cells of normal and malignant tissues were obtained. Figures 12 and 13 present the images obtained for the Adenocarcinoma and Pleomorphic Carcinoma cultured cells. As can be seen, there is a significant cellular variability within the two types of cell cultures. The cell types found in each flask have similar morphology independently of histological subtypes, either neoplastic or normal. Moreover the cellular concentration was preponderant and even exuberant in malignant cells cultures.

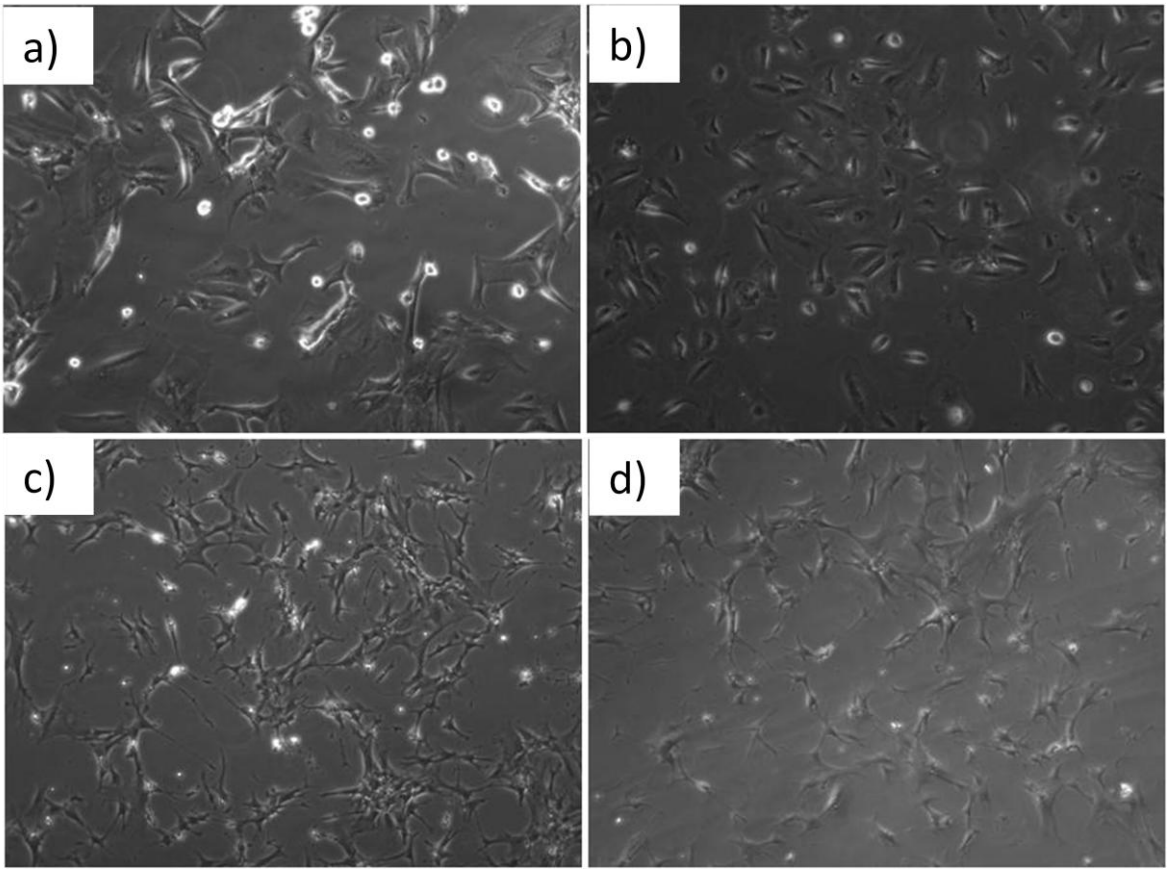

Figure 12: a) and b) cells from primary cultures of pulmonary parenchyme; c) and d) from adenocarcinoma mixed type; dark field X100

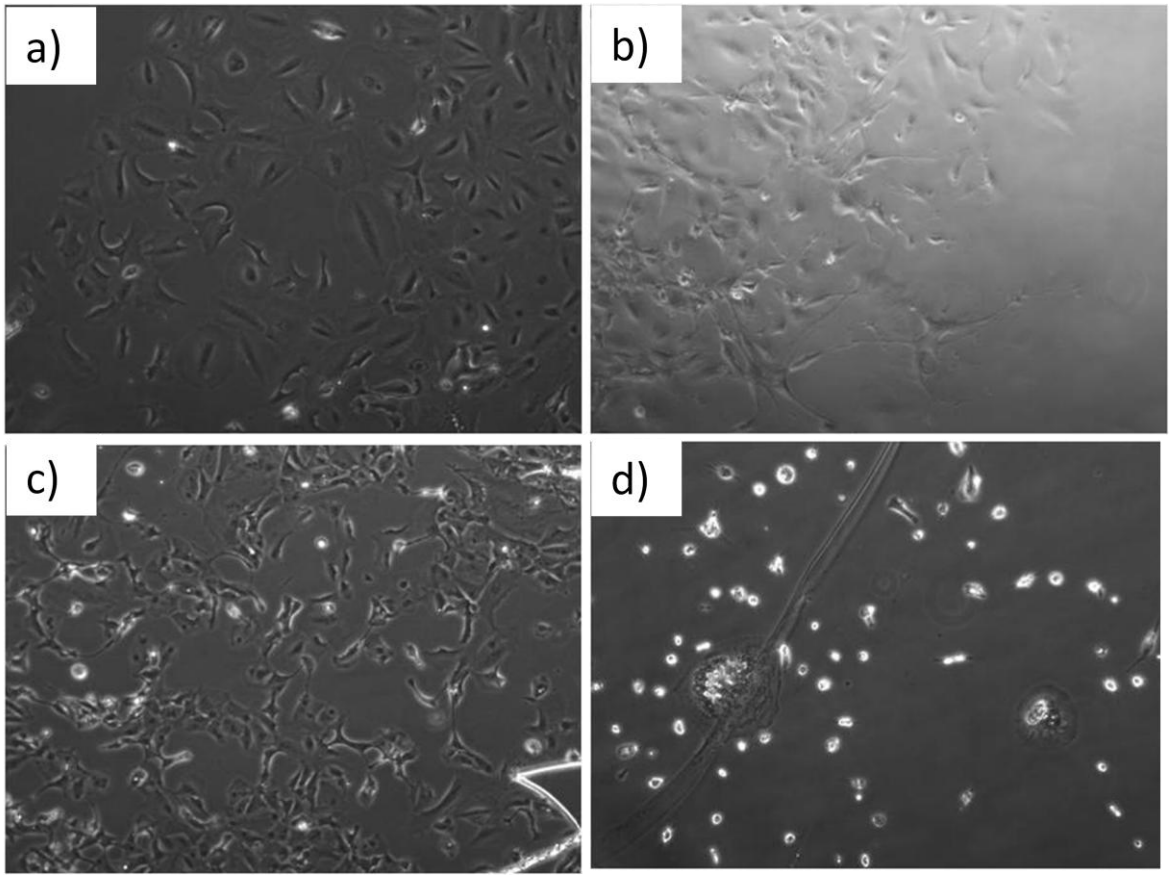

Figure 13: a) and b) cells from primary cultures of pulmonary parenchyme; c) and d) from Pleomorphic Carcinoma of the lung; dark field X100

4.2 Cell Morphology and Immunophenotype

Cell morphology and cellular aggregates were already visualized in dark field and then re-evaluated after immunohistochemical staining. Table 4 summarizes the registry of the observations. The registered different cell types were obtained either in pulmonary parenchyme (PP) or in pulmonary tumor (PT) tissue. The cells presented isolated as fibroblasts, small cells with small nuclei and scarce cytoplasm, or large cells with considerable cytoplasm and what we called, stellate cells when exhibiting dendritic-like cytoplasm. The small cells were often aggregated and then referred as morules. All cases showed to be a mixture of the different observed cell types. The relative quantities of the different cell types were variable, as validated *grosso modo* under the microscope. As can be seen in case Figures 12 and 13 the observed main types of cells: (i) fusiform cells with small and regular nuclei, as fibroblasts, (ii) polygonal stellate shaped cells with large nuclei and small nucleoli, and (iii) cell clusters of small cells forming morules with nuclear regularity, are represented, after immunohistochemical (IMC) staining (Figure14).

Table 4: Morphology and immunohistochemical analysis of the primary cell cultures

Histological typing	Cell lines	CK7	TTF1	CK5.6.18	Cell morphology
Adenocarcinoma mixed type	PP1	pos	pos		small & large cells
	PT1	pos	pos		small & large cells
Adenocarcinoma mixed type	PP2	pos	pos		small & large cells
	PT2	pos	pos		small & large cells
Adenocarcinoma mixed type	PP3	pos	pos		small & large cells
	PT3	pos	pos		small & large cells
Adenocarcinoma mixed type	PP4	pos	pos		small & large cells
	PT4	pos	pos		small & large cells
Lymphoepithelial carcinoma	PP5	pos			stelate cells
	PT5	neg			fibroblasts
Pleomorphic carcinoma	PP6	neg	pos		fibroblast & morules
	PT6	pos	neg		stelate cells & morules
Acinar adenocarcinoma	PP7	pos	neg		stelate cells & morules
	PT7	neg	pos		stelate cells & morules
Acinar adenocarcinoma	PP8	pos	neg		stelate cells
	PT8	pos	neg		stelate cells
Adenocarcinoma mixed type	PP9	pos	neg		stelate cells
	PT9	pos	neg		stelate cells
Squamous cell carcinoma	PP10			neg	fibroblasts
	PT10			neg	fibroblasts
Pleomorphic carcinoma	PP11	pos			stelate cells & fibroblast
	PT11	neg			stelate cells & morules
Adenocarcinoma mixed type	PP12	pos	neg		stelate cells & morules
	PT12	pos	neg		stelate cells & morules
Squamous cell carcinoma	PP13		neg	neg	stelate cells & morules
	PT13		neg	neg	stelate cells & morules
Squamous cell carcinoma	PP14			pos	stelate cells & morules
	PT14			pos	stelate cells & morules
Adenocarcinoma mixed type	PP15	neg	neg		stelate cells & morules
	PT15	pos	neg		stelate cells & morules
Squamous cell carcinoma	PP16			pos	stelate cells & morules
	PT16			pos	stelate cells
Squamous cell carcinoma	PP17			pos	stelate cells & morules
	PT17			pos	stelate cells
Adenocarcinoma mixed type	PP18	pos	pos		stelate cells & morules
	PT18	pos	neg		stelate cells
Squamous cell carcinoma	PP19			pos	fibroblasts & stelate cells
	PT19			neg	fibroblasts & stelate cells
Adenocarcinoma mixed type	PP20	pos	neg		stelate cells & morules
	PT20	pos	pos		stelate cells & morules
Pleomorphic carcinoma	PP21	neg			fibroblasts & stelate cells
	PT21	neg			fibroblasts & stelate cells
Pleomorphic carcinoma	PP22	neg			fibroblasts & stelate cells
	PT22	neg			fibroblasts & stelate cells

PT- Pulmonary Tumor; PP- Pulmonary Parenchyme; pos- positive; neg- negative

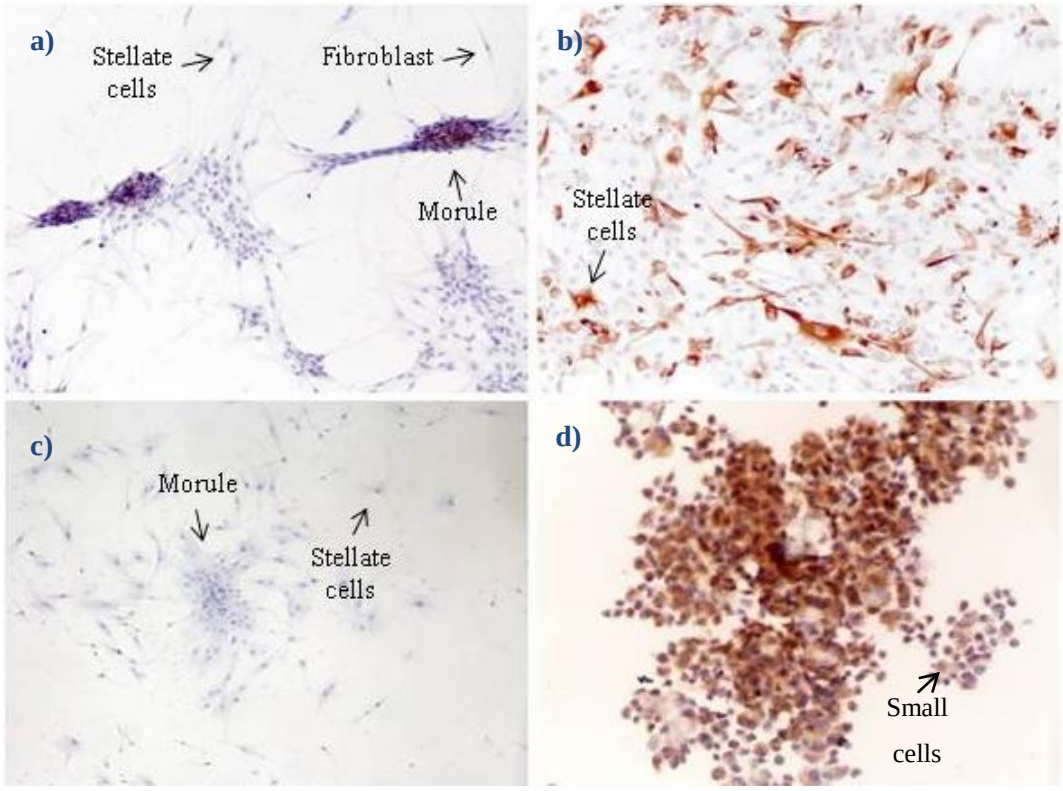

Figure 14 Immunochemistry of the cell culture (a) TTF1 X100; b) CK5.6.18 X100; c) TTF1 X40; d) CK7 X200

On the whole, cultures were established from 6 cases of Epidermoid Carcinoma (or Squamous Cell Carcinoma), 5 cases of Large and Pleomorphic Carcinoma and 11 cases of Adenocarcinomas. It was found that all three types of Carcinomas presented stellate cells, small cells forming morules, while fibroblasts were only developed in Epidermoid Carcinoma, Large cell and Pleomorphic Carcinomas (Table 5).

As shown, morula forming cells were TTF1 negative while the positive counterpart (TTF1+) was just expressed in adenocarcinoma cells; CK7 was not expressed in cells of epidermoid origin. All small and large cells of Adenocarcinomas expressed CK7. The same expression was observed in stellate cells of Adenocarcinomas. However, the stellate cells of Pleomorphic Carcinomas were CK7 negative. Moreover, morules of either Pleomorphic Carcinomas and Adenocarcinomas expressed CK7. Finally, concerning the Epidermoid Carcinomas cells, the highweight molecular citokeratins 5.6.18 were expressed. Fibroblasts and stellate cells did not express cytokeratines while morules showed positivity (Table 6).

Table 5: Morphology and Immunohistochemical Analysis of Tumoral Cells

Epidermoid (6)	Fibroblasts (1)	CK5.6.18-
	Fibroblasts & stellate cells (1)	CK5.6.18-
	Morules & stellate cells (2)	TTF1-/CK5.6.18-; CK5.6.18+
	Stellate cells (2)	CK5.6.18+
Large cell & Pleomorphic (5)	Fibroblasts (1)	CK7-
	Fibroblasts & stellate cells (2)	CK7-
	Morules & stellate cells (2)	CK7+/TTF1-; CK7 -
Adenocarcinoma (11)	Small cells & large cells (4)	CK7 +/ TTF1 +
	Morules & stellate cells (4)	CK7+/TTF1- ; CK7-/TTF1+; CK7+/TTF1+
	Stellate cells (3)	CK7+/ TTF1 -

Cell cultures obtained from pulmonary parenchyme collected away from the neoplasias were also studied and submitted to the same procedures (Table 6).

Table 6: Morphology and Immunohistochemical Analysis of cultures of Pulmonary Parenchyme Distant from each Tumor

Epidermoid Carcinomas	Fibroblasts (1)	CK5.6.18- (1)
	Fibroblasts & stellate cells (1)	CK5.6.18+ (1)
	Morules & stellate cells (4)	CK5.6.18- (1); CK5.6.18+ (3)
Large cell & Pleomorphic	Fibroblasts & stellate cells (3)	CK7+ (1); CK7- (2)
	Stellate cells (1)	CK7+ (1)
	Fibroblast & morules (1)	CK7-/TTF1+ (1)
Adenocarcinoma	Small cells & large cells (4)	CK7 +/ TTF1 + (4)
	Morules & stellate cells (7)	CK7+/TTF1- (6); CK7-/TTF1- (1)

The primary cultures has brought some success and these advances may be useful in the future for the development of an in vitro cell culture model, allowing lung cancer cells at different stages of transformation to be studied. This type of culture could help to generate biomarkers for the early detection of lung cancer (Wu, 2004).

The epithelial cells are of plastic nature, being able to respond and adapt to micro-ambiental stimuli, possibly by alteration of form, proliferation rate and differentiation state. Under some circumstances, the epithelial cells loose E-cadherin and acquire mesenchimal characteristics. Both effects facilitate cellular mobility and adaptation to extracellular matrix, a process called epithelium mesenquimal transistion (EMT). Recent studies (Brabletz, 2010; Xiao 2010) showed evidences that EMT is implicated in disease, repair and progression of many tumors. EMT has been referred as a prognostic factor for poor outcome of cancer in distinct organs, as sarcomatous changes may increase invasive potential and result in poorer outcome (Mochizuki *et al.*, 2008).

Conversely, cancer-associated fibroblasts were shown to possess heterogeneous origins and characteristics. They originate from local resident fibroblasts and/or from marrow-derived stromal cells. However, as shown by Wang et al., cancer cells recruit fibroblasts, which produce human growth factor (HGF). In turn, this production in the tumor cell agglomerates induces EGFR-TK1 resistance in lung cancer cells (Wang, 2009).

The heterogenicity observed in our piece of work shows that it was not possible to establish single primary culture cells from surgical specimens as easily as we thought at the beginning of the work because at the difficulties in immunohistochemistry revealed as heterogeneous results in pulmonary parenchyma when compared with the neoplastic samples. The proliferated specimens obtained may consist in epithelial cell, stromal cells and cells of EMT as revealed by cell morphology. On the whole the cultures obtained in the present work, established from 6 cases of Epidermoid Carcinoma (or Squamous Cell Carcinoma), 5 cases of Large cell and Pleomorphic Carcinomas and 11 cases of Adenocarcinomas showed all four types of cells developed simultaneously as stellate cells, small cells also forming morules, Large cells and fibroblasts, these mainly in Epidermoid Carcinoma, Large cell and Pleomorphic Carcinomas (Table 3). These results suggest that the Epidermoid Carcinoma, as well as the Large cell and Pleomorphic Carcinomas may encompass a spectrum till EMT. In a recent publication, however, Pruklin *et al.,* showed that despite the high expression of EMT-associated biomarkers observed in most lung carcinoma specimens, especially in squamous cell carcinoma, neither the reduced E-cadherin nor the N-cadherin overexpression seems to be associated with a poor outcome of patients. Concerning TTF1 negativity, it was observed when morula forming cells were present in Adenocarcinomas while the positive TTF1+ cells were isolated, either Small and Large cells. TTF1 has been proven to regulate the α5-nicotinic acetylcholine receptor subunits in proximal and distal lung epithelium (Reynolds, 2010) and its mixexpression has been correlated with tobacco-related lung disease.

Considering the expression of citokeratine 7 it was not expressed in cells of epidermoid origin. All small and large cells of Adenocarcinomas expressed CK7. The same behavior was observed when stellate cells of adenocarcinoma origin were considered. However, the stellate cells

of Pleomorphic Carcinomas were negative for CK7. Moreover, morules of either Pleomorphic Carcinomas or Adenocarcinoma origin seem to mainly express CK7. Finally, concerning the epidermoid type cells, the citokeratin expressed was CK5.6.18.

When comparing immunohistochemical results obtained for normal and tumoral cultured cells, there are some clear differences: in contrast with what was observed for the tumoral cell specimens, in normal tissue cultures, TTF1 was not expressed when belonging to epidermoid carcinoma. Independently of the type of cells, the epidermoid specimens only express the citokeratine CK5.6.18, with fibroblasts and morules expressing the negative counterpart and stellate cells the positive one.

In this work it was not possible to establish the histologic typing of the tumours after cellular cultures but mixtures of different cell types. Nevertheless, the present work showed that EMT may occur in these cellular cultures and some tumour cells characteristics printed that by Stellate and Large cells may be in that direction. Nevertheless, it is evident that the process of establishing cell cultures from fresh tissue still requires to be more optimized. It would be interesting, for instance, to infer if the use of collagen would in fact lead to the growing of more epidermoid cells as Epidermic Carcinomas facilitate fibroblasts growing.

In resume, there is still a lot of work to be done and the processes need to be optimized further. Hopefully, however, the herein presented results constitute an interesting starting point for more profound studies, concerning the definition of basal cells expression in Bronchial-Pulmonary Carcinomas in order to understand the Clinical meaning of EMT, after clean distinction from what may be understood as normal.

4.3 Cytogenetic characterization of the lung cell line A549

Chromosomes analysis has been a routine method for studying tumor genetics and for searching tumor-related genes. To check what type of chromosomal alterations existed in the lung cell line A549 50 cells metaphases were analyzed by GTG and various cariograms were realized.

This line was initiated in 1972 by Giard, and collaborators through explant culture of lung carcinomatous tissue from a 58-year-old Caucasian male. Further studies by Lieber, revealed that A549 cells could synthesize lecithin with a high percentage of desaturated fatty acids using the cytidine diphosphocholine pathway. According to the American Type Culture Collection (ATCC) this is a hypotriploid human cell line with the modal chromosome number between 64 and 67. Nevertheless, analyses performed in our lab revealed that the cariogram of this cell line presents a variation between chromosomes 58 and 65 in the metaphases analyzed (Table 7). The ATCC also refers the existence of two Y and two X chromosomes, being possible the occurrence of 40% loss

of one Y chromosome in the analyzed metaphases. In the present work the occurrence of two X chromosomes was confirmed while only one Y chromosome was observed.

Furthermore, the ATCC refers the occurrence of structural chromosomic changes such as chromosome derivatives der(6)t(1;6)(q11;27), and delections del(2)(q11) and del(11)(q21). It seems that there are three homolog chromosomes being that the deletion is only present in one of them. The break points seem to occur in those regions. Moreover, these break points should be confirmation by other methods such as Fluorescent in situ Hybridization (FISH).

The analysis performed on the metaphases also revealed the presence of two chromosomes but their constitution is unknown requiring additional studies.

Table 7: Distribution of the chromosome complement per number metafases analyzed

Chromosomes number	# cell
58 chromosomes	**7**
59 chromosomes	**12**
60 chromosomes	**5**
61 chromosomes	**7**
65 chromosomes	**19**

In Figure 15 there are some examples of cariograms obtained for the cell line A549. It is apparent that this line presents a complex cariogram with numerous chromosomal aberrations abnormalities. In order to get a better cytogenetic characterization of this cell line, it is required an exhaustive study by using more specific techniques as for example Fluorescent in situ Hybridization (FISH), Comparative Genomic Hybridization and array-CGH.

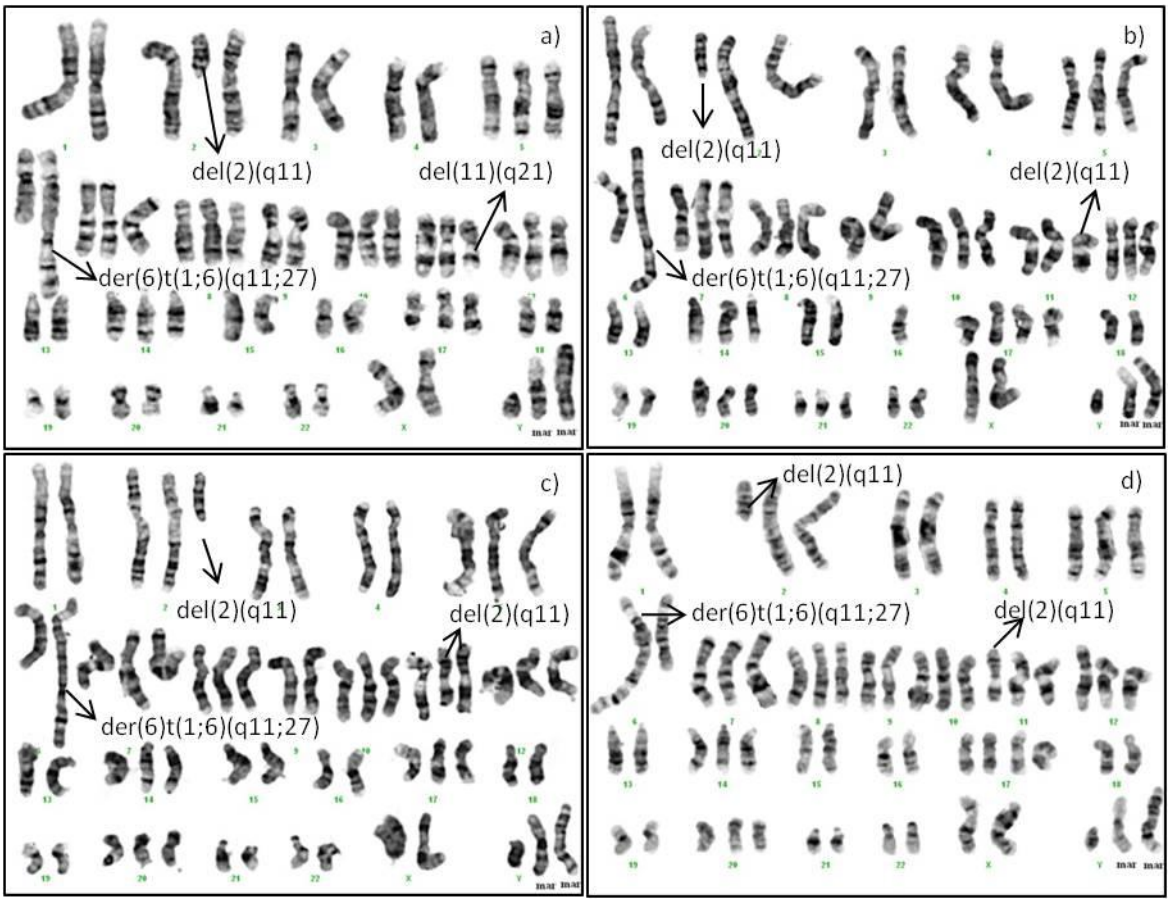

Figure 15: Examples of some cariograms of the line A549 with 58 chromosomes (a), with 60 chromosomes (b) and (d) 59 chromosomes (c). Some cytogenetic alterations are marked

4.4 Metabolic studies of A549 cells by NMR spectroscopy

4.4.1 Metabolic profile by ^{1}H HRMAS NMR

Before analyzing the effects of the external stimuli, namely the exposure to CDDP and ionizing radiation, the metabolic behavior of the untreated control cells over the experiment time was noted and, subsequently, taken as reference for the evaluation of the external stimuli effects. The effect of incubation was evaluated over time up to 48 h. Comparative inspection of the spectra of controls at 0 and 48h are presented in Figure 16 and enables some variations to be identified. Note that the aromatic regions of the spectra are not presented as no spectral change was evidenced.

To substantiate the peak assignments of the one-dimensional (1D) spectrum, a two-dimensional (2D) measurement was also conducted for the initial cell sample which is shown in Figure 17, (a) and (b) for the 0 – 6.5 and 6.6 – 9.1 ppm spectral regions, respectively. The

combination of the 1D and 2D experiments allowed assigning extensively several signals despite the high spectral complexity. The spectral assignments performed are listed in Table 8.

Table 9 summarizes the main spectral effects observed when visual comparisons are performed over time (0 → 12h, 12h → 18h; 18h → 24h and 24h → 48h). As can be seen, the spectral changes promoted by cell incubation are not a linear process over time. For instance, comparing the spectra recorded at 0 and 12h of incubation it is observed that there is an intensity decrease of the signal associated to the CH_2 lipidic groups (1.29 ppm). However, this effect is reversed by increasing further incubation time, reaching its initial intensity after 24h of incubation. A similar effect is observed for the peak at about 3.21 ppm, which is related to choline (Cho) metabolite. The content decrease observed for PC (3.23.ppm) probably contributes to the recovery of the Cho content. Finally, the spectral evidences obtained indicate that the temporal behavior of the peaks related to glutamate (2.35 ppm) and glutathione (GSH; 2.56 ppm) metabolites opposes the one observed for both mobile lipids and Cho. In fact, both metabolites present an initial content increase, followed by a significant and gradual decrease that starts after 12h of incubation.

The decrease of the content of glutamate, GSH and PC after 48h of incubation is in accord to the results reported by Duarte *et al.,* (Duarte *et al.*, 2010) for the MG-63 osteosarcoma cells. However, opposing those results, the present spectral comparisons did not evidence aminoacid and myo-inositol content variation upon that time of cellular incubation.

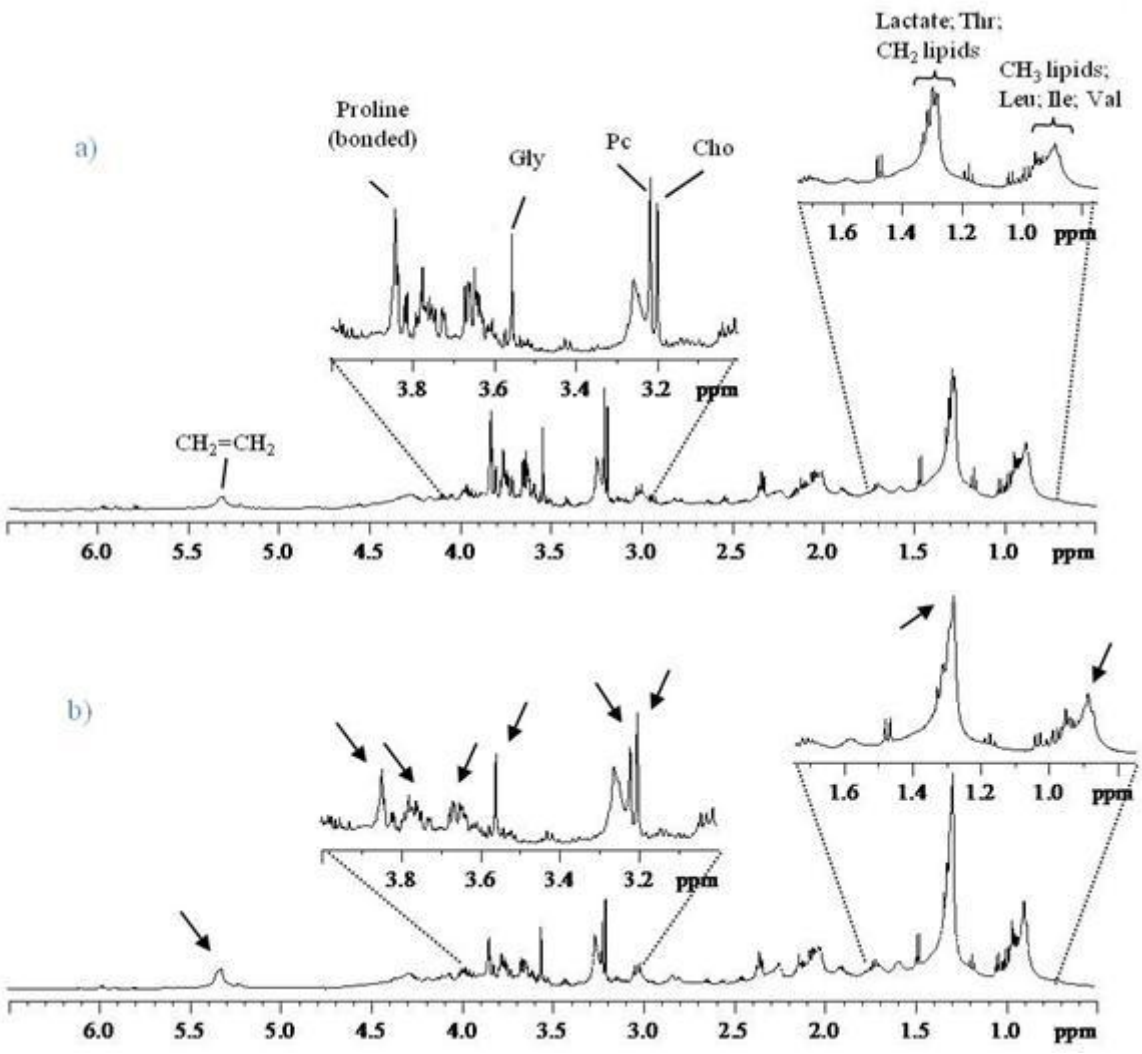

Figure 16: Average ^{1}H HRMAS spectra obtained for control cells at a) 0 b) 48hours incubation time. Arrows indicate the most visible changes

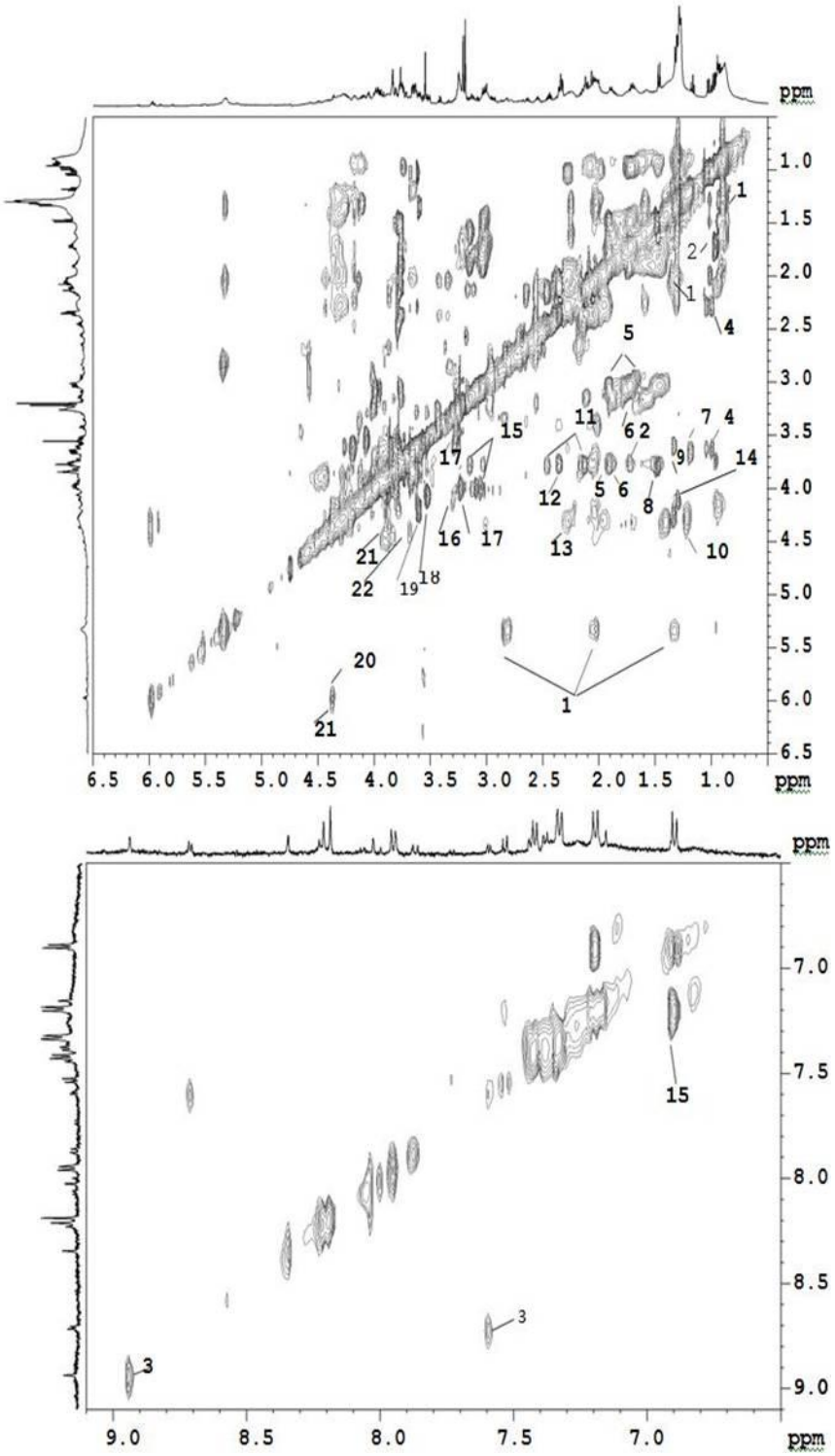

Figure 17: Expansions of 500 MHz 2D a) TOCSY (0.5-6.6 ppm) and b) TOCSY (6.5-9.1) spectra of fully lysed A549 cell line. Peak numbers correpond to metabolites identified in Table 8

Table 8: Assignment of the 500 MHz 1D and 2D HRMAS NMR spectra of fully A549 cell line

Number	Metabolite name	δ ^{1}H (ppm)
1	Fatty acyl chains (lipids)	0.90/0.96; 1.29; 1.58; 2.04/2.08; 2.25; 2.81; 5.32
2	Leucine	0.96 (d); 0.97 (d); 1.7; 1.72; 3.74 (t)
3	Nicotinamide	7.60/7.63 (q); 8.25/8.34 (d); 8.94/9.08 (s); 8.72/8.82 (d)
4	Valine	0.99 (d); 1.04 (d); 2.28; 3.62
5	Lysine	1.47; 1.73; 1.92; 3.03 (t); 3.76 (t)
6	Arginine	1.69; 1.92; 3.24 (t); 3.78
7	Ethanol	7.5; 1.19 (d); 3.66 (q)
8	Alanine	1.48 (d); 3.78
9	Treonine	1.34 (d); 3.59 (d); 4.26
10	Treonine bonded	1.22 (d); 4.26
11	Glutamine	2.15; 2.45; 3.79
12	Glutamate	2.06; 2.13; 2.35; 3.78
13	Glutamate bonded	1.95; 2.04; 2.3; 4.3
14	Lactate	1.33; 4.12
15	Tyrosine	3.20 (dd); 3.05 (dd); 3.94; 6.89 (d); 7.18 (d)
16	Phenilalanine	3.13; 3.27; 3.99; 7.32; 7.37; 7.42
17	*myo*-inositol	3.28; 3.54; 3.62; 4.07
18	Choline	3.21 (s); 3.53; 4.07
19	Phosphocholine	3.23 (s); 3.62; 4.19
20	UDP/UTP	5.97; 7.97
21	Inosine/Adenosine	3.86; 4.28; 4.44; 4.78 (t); 6.10 (d); 8.23 (s); 8.36 (s)
22	Glycerophosphocholine (GPC)	3.23; 3.71; 4.33

Table 9: Metabolites variations observed in control cells (↑ increase; ↓ decrease; ↑ = increases until equalizing t = 0h; = equal to t = 0h)

Metabolites	0-12 h	12-18 h	18-24 h	24-48 h
CH_2 (mobile lipids)	↓	↑	↑=	=
Choline	↓	↑	↑=	=
Phosphocholine	↓	↓	↓	↓
Glutamate	↑	↓	↓	↓
Glutathione	↑	↓	↓	↓

On the whole, the initial metabolite content variations described above may be explained as being related with a cellular adapting process to overcome the consequences of the high proliferation rate. However, with increase of incubation time both cellular density increase in the flasks and decrease of the nutrients availability in the medium promotes a new stressing effect in the samples. This stress effect may induce cellular death that justifies the increase of the contents in mobile lipids and Cho after an initial period of increase. In fact, as referred previously the increase of those cellular metabolites as well as the decrease in PC have been widely correlated to cellular apoptosis promoted by a variety of distinct external stimuli (Merz and Serkova 2009).

The presented spectral observations and corresponding metabolite content variations are of great relevance for the subsequent studies related to the effect of CDDP addition and cell irradiation. In fact, the presented results suggest that after the initial 12h of incubation significant cell stress is expected to occur due to cell incubation, and not due to any of the other external stimuli applied. In other words, the analysis of the spectral changes promoted by both CDDP addition and irradiation, and consequently the corresponding metabolic explanations, has to be performed with special care.

4.4.2 Metabolic response to cisplatin

Figure 18 shows the ^{1}H HRMAS NMR spectra of cellular line A549 before and 48h after treatment with 50 μM CDDP solution. The spectrum of the control cells (*i.e.*, after 48h without treatment with CDDP) is also included. Some peaks assignments, made on the basis of Table 8, are indicated. Comparison of the two spectra presented shows that the intensity of several peaks is significantly affected after 48h of CDDP treatment. For instance, the CH_2-related peak at 1.29 ppm is clearly intensified. The same effect is observed for the peak centered around 5.98 ppm which has been related to UDP. Contrariwise, the doublets centered at about 5.79 ppm and 7.53 ppm, assigned

to uracil, and the peaks at ca. 8.94 ppm and 8.70 ppm (doublet), assigned to niacinamide, almost disappear.

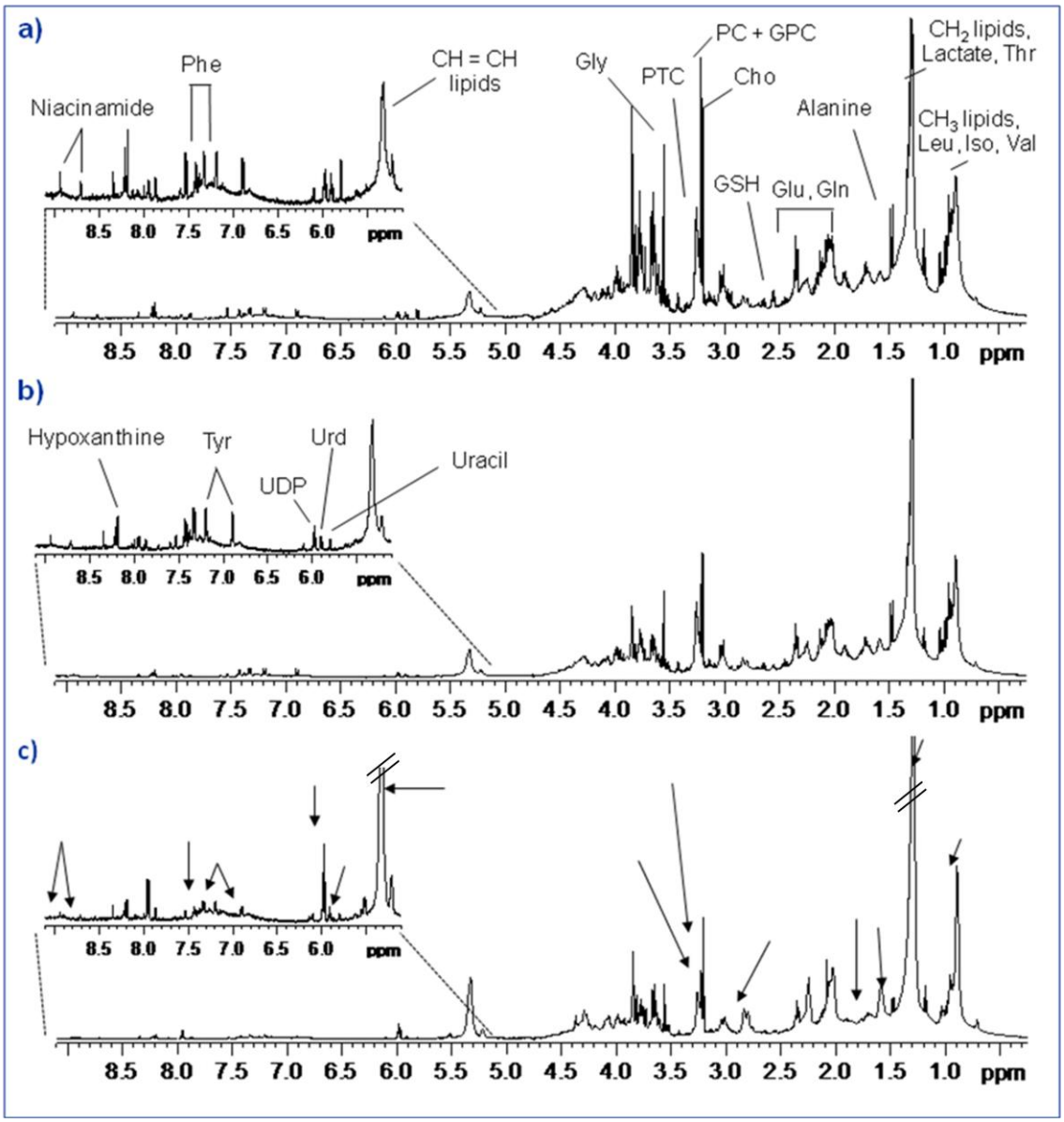

Figure 18: Average 1H HRMAS spectra obtained for control cells at a) 0 b) 48 hours, and c) cells exposed to 50 µM CDDP for 48 hours. Arrows indicate most visible changes observed after treatment with CDDP

In order to infer the temporal effect of CDDP exposure, the intensity variation of several peaks as previously performed for the effect of the incubation time (0 → 12h, 12h → 18h; 18h → 24h and 24h → 48h). The results of the evaluation are summarized in Table 10. As for the effect of incubation time it can be seen that the temporal effect of CDDP exposure on the content of the majority of the identified metabolite is not a linear continuous effect.

Starting with the analysis of the first 12h of exposure to CDDP, it can be seen that the effect observed generally opposes the effect of simple cellular incubation (Table 9 vs. Table 10). In fact, in the first 12h of exposure, CDDP intensifies the peaks related to mobile lipids (1.29 ppm), Cho (3.20 ppm) while the signals ascribed to glutamate and glutathione (2.35 and 2.56 ppm, respectively) denote a slight intensity decrease (particularly small in what concerns glutamate).

Table 10: Metabolites variations observed in CDDP-treated cells (50 μM) (↑ increase; ↓ decrease; = equal to t = 0h; (a) slight; (b) inferior to initial value; (c) almost invisible; the number of arrows is proportional to the variation observed)

Metabolite	0-12 h	12-18 h	18-24 h	24-48 h
CH_2 (mobile lipids)	↑	↓=	↑↑↑	↑↑↑
Phosphocholine	↓	↓	↓↓	↓↓
Glycerophosphocholine	↑	↑	↑	↓
Choline	↑ (a)	↑	↓↓ (b)	↓↓ (b)
Glutathione	↓	↓↓	↓↓↓	↓ (c)
Glutamine	↑↑	↑↑↑	↓↓↓ (b)	↓↓↓
Glutamate	↓ (a)	=	↓↓↓	↓↓
Alanine	↓ (a)	↑	↓↓↓ (b)	↓↓↓
Leucine	=	↑↑	↓↓ (b)	↓↓↓
Tyrosine	=	↑↑	↓↓↓ (b)	↓↓↓
Phenylalanine	=	↑↑	↓↓ (b)	↓↓↓
Valine	=	↑↑	↓↓ (b)	↓↓↓
Glycine	↓↓	↑=	↓↓↓	↓↓
Hypoxanthine	↓↓	↑↑ (b)	↓↓↓	=
Inosine/Adenosine	↑↑	=	↓↓	↓↓↓ (b)
Niacinamide	↓ (a)	=	↓↓	↓↓↓
Uracil	↓↓	=	↓↓↓	↓↓↓ (c)
UDP/UTP	↑↑	↑↑	=	↑↑↑

In contrast to what was observed for the effect of incubation time, the initial 12h of drug exposure also affect significantly the glutamine content as judged by the intensity increase observed in the peak at 2.45 ppm. This effect may be explained as an initial cellular tentative to protect the cell from the stress promoted by the drug, namely induction for apoptosis. According to

Matés *et al.*, (Matés *et al.*, 2002, glutamine promotes protein synthesis not only by furnishing energy but also by promoting the gene transcription.

Other significant variations are also observed on the peaks related to inosine and adenosine (8.34 ppm for both metabolites and 8.23 ppm for the later one). Both metabolites are produced as degradation products of pyridine and purine nucleotides. But they are also known to interfere in the so-called salvage reactions being utilized in the synthesis ATP and GTP (Ashihara *et al.*, 2008). In a publication Módis *et al.*, showed that pretreatment of cells with acute tubular necrosis with adenosine and inosine significantly protects the cells subjected to oxygen-glucose deprivation against the fall in cellular ATP content. In fact, according to the authors this protection is related to both the interaction of the metabolites with the cell surface adenosine receptors and adenosine conversion to ATP (Matés *et al.*, 2002).

Finally, the content of most of the detectable aminoacids remains more or less unaffected by CDDP in the initial 12h of exposure. The only exception is glycine which content seems to be significantly decreased judging by the significant intensity decrease observed for the signal at 3.56 ppm.

Based on all these observations it seems that the first 12h of drug exposure are not critical for cellular survival. The necessary requirements are probably satisfied by increasing the uptake of glutamine from the medium. By this way, the cell not only satisfies its needs of energy but also guarantees the content of glutamate (recall almost unaffected), a precursor for the synthesis of the antioxidant metabolite glutathione that is, probably, being extensively used to overcome drug-related stress.

Increasing incubation time in the presence of the drug generally inverts the tendencies observed in the first 12h of many metabolites. In the subsequent 6h (12h → 18h) there seems to be a significant content increase of several identified aminoacids (Table 10). For instance, the peaks related to alanine (duplet around 1.48 ppm) and glicine (3.56 ppm), which denoted a intensity decrease in the first 6h (relatively significant in the later case), are intensified reaching or even overcoming the initial intensity (t =0h). Other signals related to valine (duplet around 1.04 ppm), phenylalanine (several peaks in the 7.32-7.42 ppm region), tyrosine (two duplets at 6.89/6.90 ppm and 7.18/7.20 ppm) and leucine (0.96 ppm and 1.70 ppm) are also significantly intensified. This spectra effect is, however, reversed when incubation in the presence of the drug is extended beyond the 18h. In fact, after 18h of incubation (18h → 24h), the intensity of the NMR signals related to those aminoacids denotes a pronounced decrease. This effect seems to be irreversible and continual with the concentration dropping drastically after 24h and 48h of incubation. The generality of these temporal behavior of the different NMR signals has been already reported by Huang *et al.*, for the

same cell line (A549) submitted to a significantly lower CDDP concentration (30 μM) (Huang *et al.*, 2003).

At this stage it is important to refer that intracellular concentration of leucine, for instance, has been considered to represent a balance between several factors such as intracellular protein catabolism and the mechanism of its removal by oxidation and/or protein synthesis (Norton and Layman, 2006). Moreover, it has been shown that leucine has a direct effect in the regulation of the mechanisms involved in protein synthesis (Vianna *et al.*, 2010). Being leucine one of the essential aminoacids (*i.e.*, is not is not synthesized by the cells), its concentration enhancement is probably related to an intensification of the catabolic pathways of proteins with the aim of energy production. This enhancement also explains the increase observed for the intracellular contents of the other aminoacids in the initial 24h period. However, continuing incubation in the presence of CDDP leads to the continuing degradation of those aminoacids and thus the situation tends to the exhaustion of their cellular content.

Similar explanation applies for the content variation denotes by other metabolites as judged by the intensity variation of the corresponding NMR signals. For instance, after an initial intensity increase denoted by the signal related to glutamine (2.45 ppm), which extends up to 18h of incubation, a pronounced intensity decrease is observed by extending incubation. The contents of both inosine and adenosine are also significantly decreased after the initial increase (0h → 12h) and stabilization (12h → 18h). Moreover, the peaks related to niacinamide (a metabolic precursor of NAD and NADP) (Ashihara *et al.*, 2008) at 8.94 and 8.71 (duplet), which in the initial 18h only denoted a slight intensity decrease, is significantly affected after that time of incubation becoming almost invisible. Similarly, the content of GSH is also progressively decreased, becoming the peak at 2.56 ppm almost invisible after the 48h of incubation. Opposing the intracellular concentration variations described for many cellular metabolits, the content of mobile lipids is significantly increased after 18h of incubation. In fact, the intensity of the peak at 1.29 ppm is drastic and progressively increased in the period of 18 – 48 h of incubation.

Based on the described spectral changes it can be concluded that in the initial 18h of incubation in the presence of CDDP the cell develops mechanisms attempting to overcome the stress promoted by the drug. The uptake of glutamine is increased in order to balance the level of glutathione that is being extensively used to control the oxidative stress that occurs, as indicated by the slight decrease of the niacinamide (NAD and NADP precursor) level. Simultaneously, the energetic requirements are guaranteed by enhancing the contents of both inosine and adenosine, two important metabolic precursors of ATP and GTP, and protein first and subsequently aminoacids degradation. However, with the exhaustion of those metabolites reserves the cell is no longer able to satisfy its energetic requirements and/or overcome the oxidative stress, and thus

enters in cell deaths processes. This is clearly evidences by the significant increase observed for the mobile lipids content.

To finalize it is interesting to note that in the period of 12 – 18h of incubation the cells are to some extend able to recover from the initial stressing effects promoted by CDDP. When considering the effects of incubation without drug in the same time interval (Table 9) the results show an initial decrease of the CH_2 content (0 – 12h) followed by a continuing content increase until equalization of the initial concentration. But if incubation is made in the presence of CDDP (Table 10) the opposite behavior is observed. An initial intensity increase of the peak at 1.29 ppm (0 – 12h) is followed an intensity decrease until the initial value is achieved after 18h. After that time, the CH_2 content seems to continuously increase over time suggesting that at this stage the cell death is not avoidable.

Supports to these time course changes of the metabolite content are obtained by tracing the integrated areas of the NMR peaks. Figure 19 shows the integrated areas determined for some of the NMR peaks related to some of the metabolites for which more pronounced content variation were observed by visual comparison of the control and treated cell spectra. The integrals clearly confirm the increase in the lipids content after the initial 12 h of incubation. They also confirm the considerable decrease of some other cellular metabolites, namely glutamine and glutathione, as well as of many of the aminoacids.

Multivariate analysis was also performed using the cells spectra in order to confirm the visual observations discussed above and to identify the most statistically relevant spectral changes. The Partial Least Squares regression Discriminant Analysis (PLS-DA), obtained for the spectra of controls and of CDDP-treated cells is shown in Figure 20. As can be seen, there is a relative discrimination between the two types of samples along LV1. The corresponding loadings of LV1, coloured according to Variable Importance in the Projection - VIP (Figure 21) indicate that this separation is mainly due to increased contents of lipids, glutamate, GPC and UDP in treated cells (negative LV1 Loadings) together with decreased levels of several aminoacids and inositols (positive LV1 Loadings). These content changes are mostly in line with the variations referred on the basis of visual spectral comparisons. The exceptions are the increased levels of both glutamate and GPC, which seemed to be decreased base on the direct comparison of control and treated cells spectra.

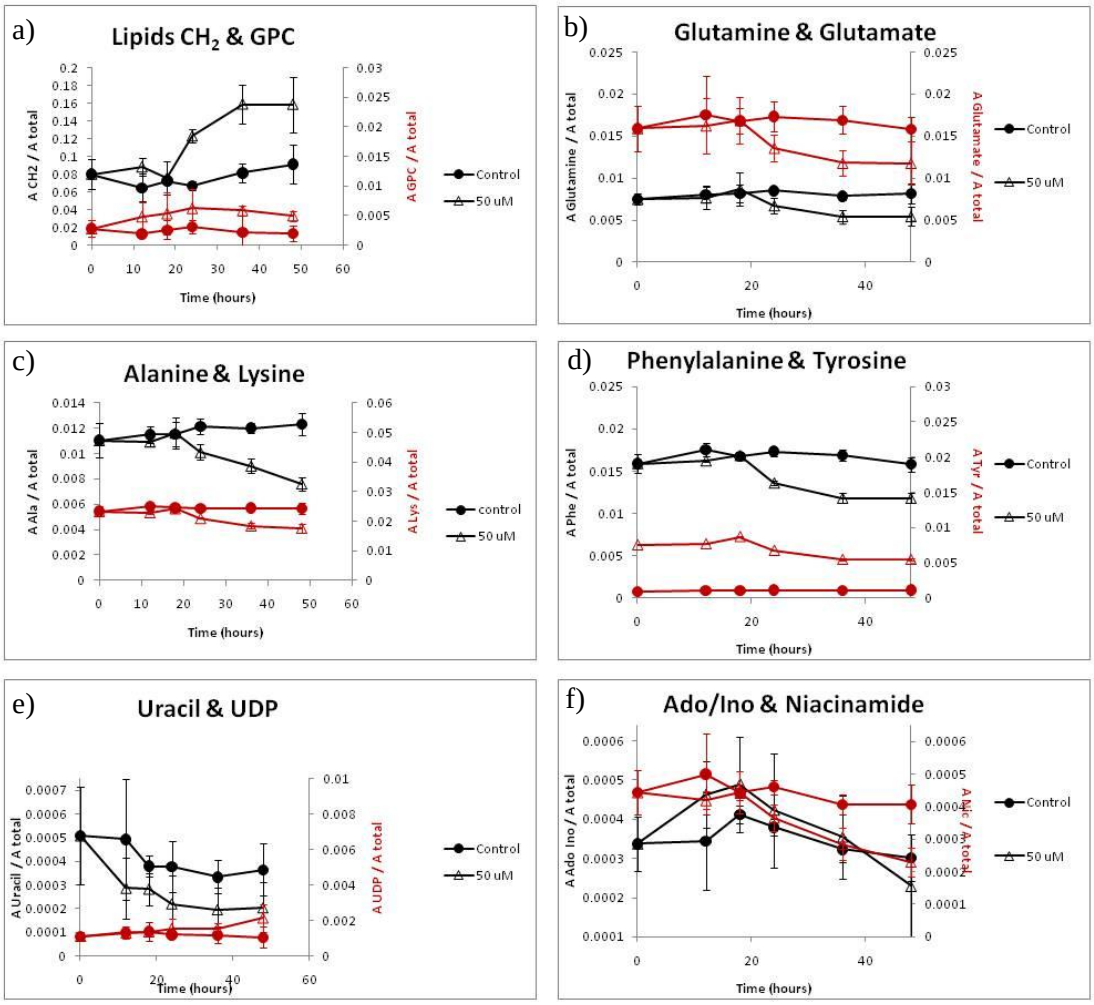

Figure 19: Plots of area ratios (to total spectral area) as a function of time of exposure to CDDP a) Lipids CH_2 (black) and Glycerophosphocholine (GPC) (red), b) Glutamine (black) and Glutamate (red); c) Alanine (black) and Lysine (red), d) Phenylalanine (black) and Tyrosine (red), e) Uracil (black) and Uridine diphosphate (UDP) (red) and f) Adenosine/Inosine (black) and Niacinamide (red)

The coloring of the LV1 loadings (Fig. 21) shows that the impact of CDDP treatment. The peaks colored in red/orange arise from metabolites presenting higher importance for the discrimination between the control and treated cells. As can be seen, the variations of the metabolite content promoted by CDDP exposure is reflected over the entire cell spectrum, in accordance to what was observed previously for other CDDP-treated cell lines (Duarte *et al.*, 2010). The most statistically relevant spectral changes are related to the peaks associated to the lipid protons. Nevertheless, the peaks related to other metabolites also denote significant variation. For instance, the contents of GPC and UDP seem to be significantly enhanced in the treated cells in

relation to the control samples. In opposition, the levels of aminoacids phenyalanine, tyrosine, lysine, alanine, leucine and isoleucine are decreased upon CDDP treatment.

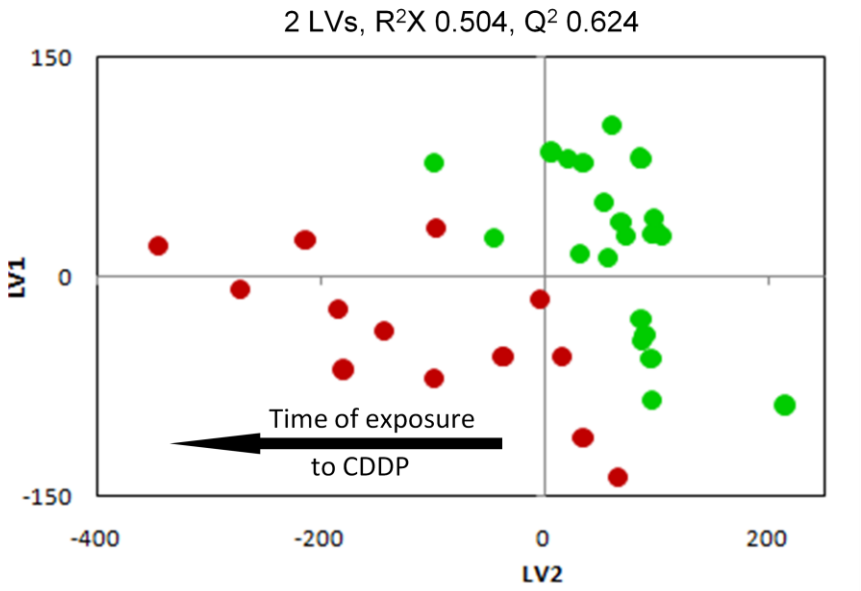

Figure 20: PLS-DA scores scatter plot of controls (•) and 50µM CDDP-treated cells (•)

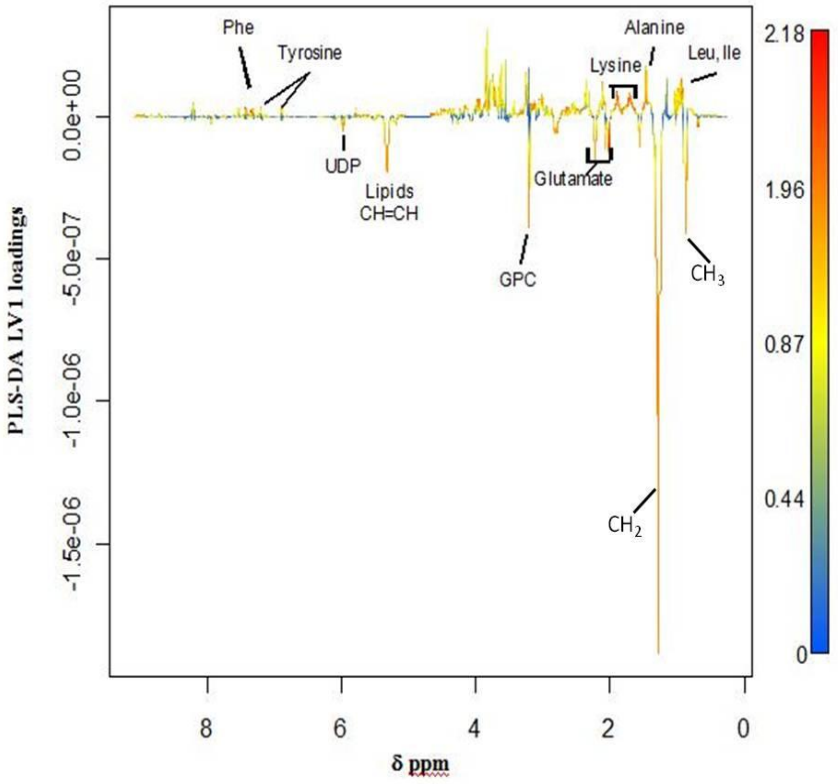

Figure 21: PLS-DA LV1 loadings with color scale reflecting the statistical relevance of each signal

On the whole, the results concerning the effect of exposure to CDDP showed a clear increase of the CH_2 lipid content, particularly after 20h of exposure. This lipid content variation has previously been observed by others. For instance, the results reported by Huang (Huang *et al.*, 2003) point to a significant increase of the CH_2/CH_3 ratio after 20h exposure of the same cell line to CDDP. The same agreement is, however, not noted for the variation of the GPC levels. According to the work of Huang (Huang *et al.*, 2003) there should be a gradual decrease of that metabolite level after treatment with CDDP. However, the present results (Fig. 21 a) do not evidence that decrease pointing, in fact, to an opposite effect, that is, a slight increase of the GPC content.

Prior works of the literature correlated the cellular level of phosphomonoesters (PME) with the cellular ability to proliferate. According to Huang (Huang *et al.*, 2003), as higher the level of PMEs as greater the cellular ability to proliferate. The present results point to a gradual decrease of the cellular content of PMEs, in particular GPC (Fig. 21). Thus, assuming the prior correlation established (Huang *et al.*, 2003) it may be concluded that CDDP has indeed some inhibitory effect on cellular proliferation.

One other CDDP effect that deserves some attention is the effect on the gluthatione cellular level. Several studies of the literature associate the strong affinity of CDDP to complex to

intracellular gluthatione molecules as one potential mechanism of cellular resistance to the platinum drug (Huang *et al.*, 2003). Moreover, metabolites such as glutamine, glutamate and GSH are involved in cellular detoxification, with both glutamine and glutamate being in the GSH synthesis pathway, as represented in Figure 11.

4.4.3 Metabolic response to ionizing radiation

Figure 22 compares the ^{1}H NMR spectra recorded for the control cells (i.e., not irradiated) ate t = 0 and 2h (a) and b), respectively) and for a cell sample 2h after being irradiated. As previously, a temporal analysis of the spectral features intensity variation was performed, considering irradiated sample up to 72h incubation after irradiation. The main intensity variations observed are summarized in Table 11.

In the second column of Table 11, the effect of irradiation is evaluated by comparing the spectra of the control and of the irradiated sample, both after 2h of incubation. It can be seen that radiation has a significant initial impact on the cellular metabolites level. For instance, the levels of the aminoacids detected are generally decreased. The level of glutamine is not affected, contrasting with the effect observed for the levels of GSH and glutamate which are significantly decreased. Simultaneously, the level of inosine and adenosine are also significantly increased upon irradiation. The correlation of these spectral effects with potential metabolic responses is not easy to establish. In general, the observations follow those observed for the initial effect of CDDP (Table 10). However, the similarities do not apply when the analysis is extended to the contents of mobile lipids and choline-containing compounds. In fact, contrasting to what is observed for the CDDP effect, radiation exposure seems to promote an initial decrease of the mobile lipids content. Simultaneously, there is a clear increase of the Cho and PC levels accomplished by a decrease of the GPC level.

Despite the initial behavior observed, the overall results clearly show that most of the metabolites recover their initial concentration 24h after irradiation (3rd column of Table 11). In fact, after that time the effects of radiation are generally overcome and reversed. The level of the identified aminoacids is increased over time, suggesting an enhancement of protein catabolism. Simultaneously, the levels of inosine and adenosine are significantly decreased giving evidences of nucleotides synthesis being enhanced. In counterpart, the level of mobile lipids is increased, but it is not evident if these effect is related to a direct effect of radiation over time or if it simply corresponds to an effect of incubation, as discussed previously in section 4.4.1.

As previously for the effect of CDDP exposure, these time-course changes promoted by irradiation find clear supports when the integrated areas of the peaks are analyzed in function of time of incubation (Figure 23). As can be seen, the results confirm the decrease of the Lipids and

the increase of the GPC levels upon radiation exposure. Moreover, the level of some aminoacids, such as Alanine, Phenylalanine, Tyrosine and to a smaller extend, Glycine, are increased. The levels of Niacinamide and the adenosine also show a tendency to increase upon radiation exposure relative to the control cells.

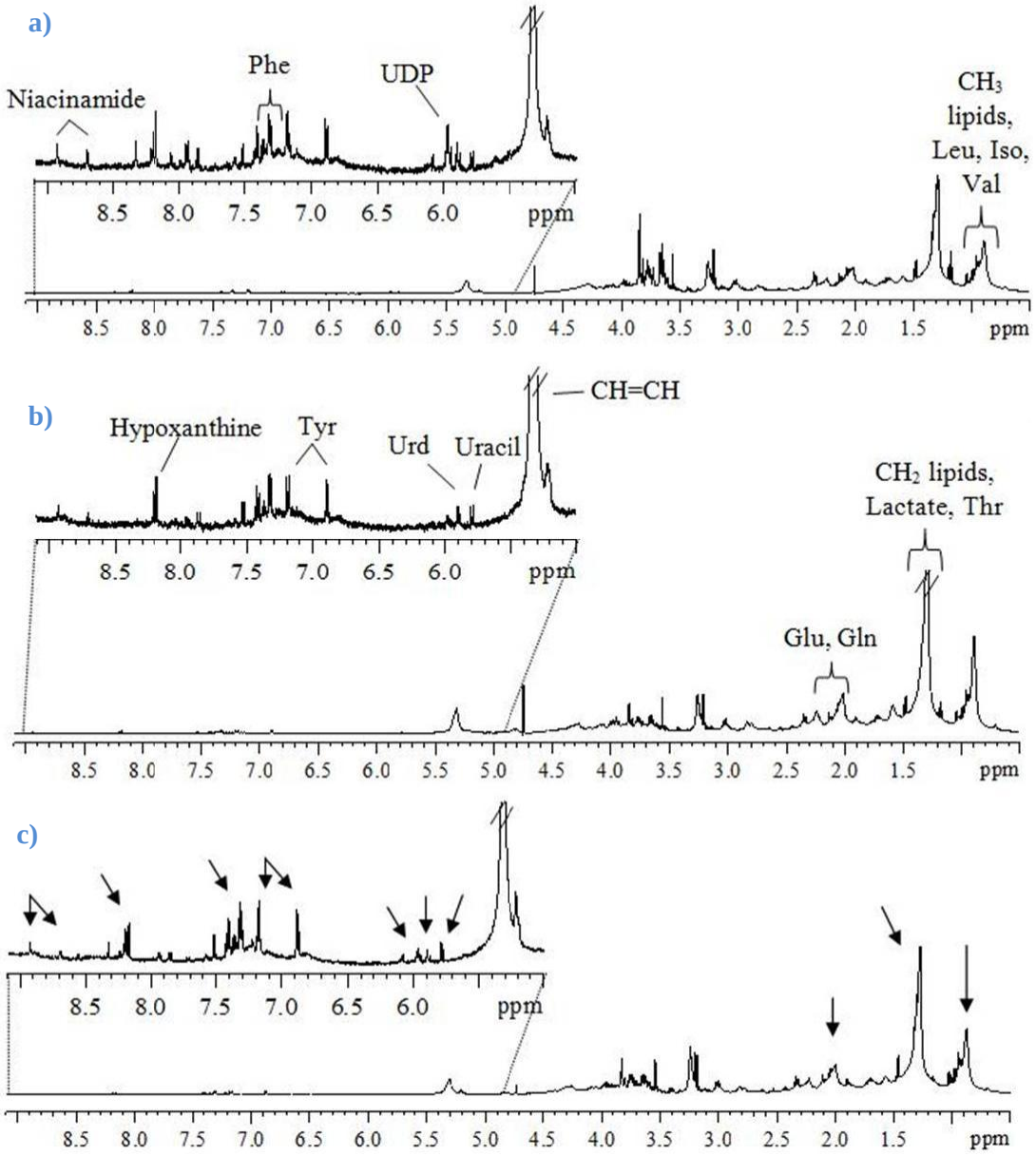

Figure 22: Average ^{1}H HRMAS spectra obtained for control cells at a) 0 b) 2 hours, and c) radiation cells for 2 hours. Arrows indicate most visible changes observed after radiation

Table 11: Metabolites variations observed in radiation cells (6 Gy) (↑ increased; ↓ decreased; = equal to t = 0h; (b) inferior to initial value; (d) superior to initial value; the number of arrows is proportional to the variation observed)

Metabolite	2h (prior/ after radiation)	2-24 h	24-48 h	48-72 h
CH_2 (mobile lipids)	↓↓	↑↑/recover	↑↑↑	=
Phosphocholine	↑↑	↓↓↓ (b)	↑	↑
Glycerophosphocholine	↓↓	=	↓/invisible	invisible
Choline	↑↑	↓ (d)	↓	↓↓
Glutathione	↑	↓↓↓ (b)	↓	↑↑
Glutamine	=	=	↓↓	=
Glutamate	↑	↓ (d)	=	↑↑
Alanine	↓↓	↑↑/recover	↑	↑
Leucine	↓	↑/recover	↑	↑
Tyrosine	↓↓	↑↑/recover	↑	=
Phenylalanine	↓↓	↑↑/recover	↑	=
Valine	↓	↑↑	↑	=
Glycine	↓↓	↑↑/recover	=	↓
Hypoxanthine	↓↓	↑ (b)	=	=
Inosine/Adenosine	↑↑	↑↑/recover	↓↓	=
Niacinamide	=	=	↓↓	=
Uracil	=	↑↑	=	=
UDP/UTP	=	↓↓	↓↓↓	=

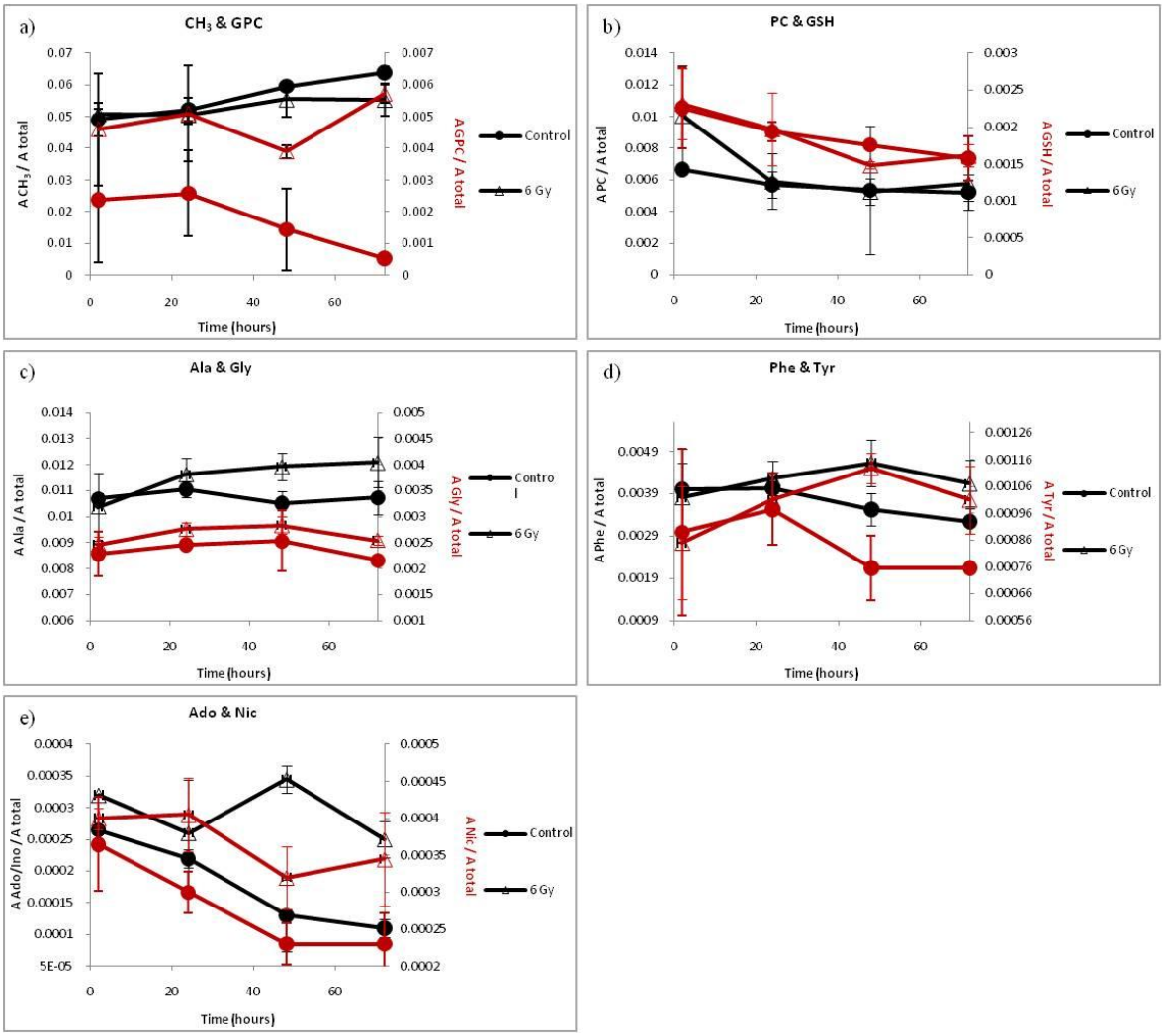

Figure 23: Plots of area ratios (to total spectral area) for a) Lipids CH_3 (black) and Glycerophosphocholine (GPC) (red), b) PC (black) and GSH (red), c) Alanine (black) and Glycine (red), d) Phenylalanine (black) and Tyrosine (red) and e) Adenosine /Inosine (black) and Nicotinamide (red) after radiation exposure time

The discriminant analysis of the least-square regression (PLS-DA), is show in Figure 24. As can be seen there is a clear discrimination between the samples submitted to the ionizing radiation (6 Gy) and the control samples along LV1. The analysis of the scores shows that the in what concerns the control samples there is a time-course effect. In other words, as time of incubation increases the score shift along the positive LV2 axis. The same effect is, however, not observed for the irradiated samples, for which the scores are spread randomly along the LV2 axis. This observation suggests that the radiation effects occur at the moment of cell exposure to radiation.

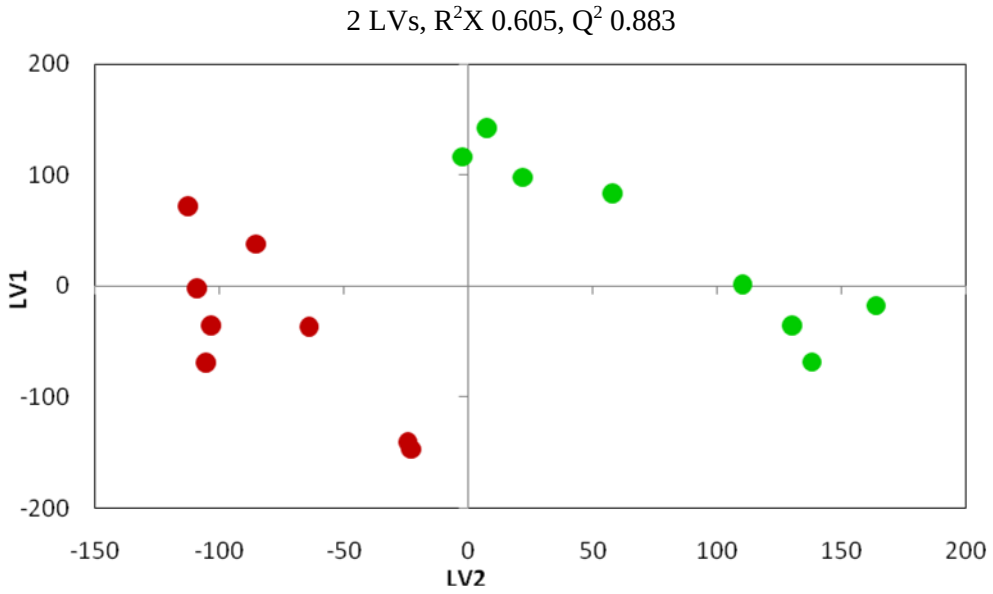

Figure 24: PLS-DA scores scatter plot of controls (•) and 6Gy – irradiation cells (•)

The corresponding LV1 loadings colored according to VIP (Figure 25) suggest that, on average, lipids are decreased in irradiated cells relative to controls, whereas several metabolites such as aminoacids, inosine, adenosine, Cho, PC and niacinamide are increased relative to the controls. In this way, it seems that exposure to a 6 Gy ionizing radiation leads to metabolite content variations that oppose the one observed for CDDP exposure. However, this conclusion has to be taken with care. In fact, it is desirable to perform more profound studies particularly concerning the effect of irradiating the A549 cells in order to draw more definite effects.

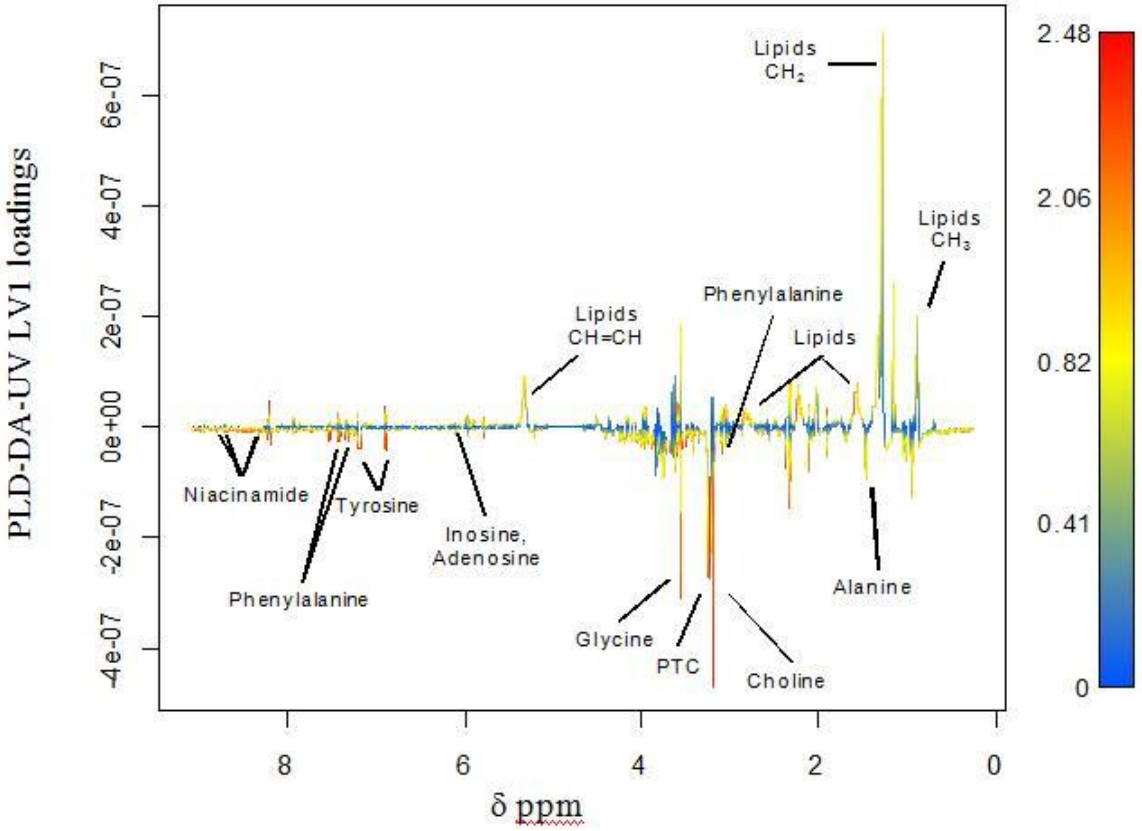

Figure 25: PLS-DA LV1 loadings with colour scale reflecting the statistical relevance of each signal

Conclusions and future perspectives

5 Conclusions and future perspectives

The heterogenicity observed in our work shows that it was not possible to establish single primary culture cells from surgical specimens as heterogeneous results in pulmonary parenchyme when compared with the neoplastic sample. Nevertheless, the present work showed that EMT may occur in these cellular cultures and some tumour cells characteristics printed that by Stellate and Large cells may be in that direction. Nevertheless, it is evident that the process of establishing cell cultures from fresh tissue still requires to be more optimized. It would be interesting, for instance, to infer if the use of collagen would in fact lead to the growing of more epidermoid cells as Epidermic Carcinomas facilitate fibroblasts growing. In summary, future studies should entail the definition of basal cells expression in bronchial-pulmonary carcinomas in order to understand the clinical meaning of Epithelium Mesenquimal Transistion (EMT), after clean distinction from what may be understood as normal.

Concerning the metabolic profiling of A549 lung cells, using ^{1}H NMR spectroscopy, the present study gave some interesting insights into the metabolic response of those cells to external stimuli, namely addition of cisplatin (CDDP) and irradiation with a 6 Gy ionizing radiation. Based on the spectral variations observed for the NMR signals related to particular metabolites it was possible to infer which metabolic pathways are potentially the most affected by each particular stimuli. It was found that within the first hours of exposure to CDDP, the cells are able to increase the uptake of glutamine probably in a attempt of overcoming the oxidative stress promoted. At the same time, production of NAD and NADP metabolites are probably increased as judged by the reduction of the niacinamide level. Moreover, in view of guaranteeing the energetic requirements the levels of the ATP and GTP precursors inosine and adenosine are enhanced as well as protein catabolism. However, with the exhaustion of the metabolic nutrients after several hours of incubation with the drug, the cell enters in processes that culminate with its death. This is clearly evidenced by the huge increase observed for the mobile lipid peak.

In what concerns the effect of radiation it is desirable to perform more profound studies to confirm the preliminary results herein presented. Nevertheless, it seems to be evident from the results obtained that the cells are able to recover quite well from the effects of the radiation in the 2h following irradiation. The preliminary results also seem to suggest that the effects of cell sample irradiation with a 6 Gy ionizing radiation leads to opposite metabolite content variations over time relative to CDDP exposure.

References

References

Alberg A and Samet J (2003) *Epidemiology of Lung Cancer*. Chest 123:21-49;

Ashihara H, Luit B, Belmonte M and Stasolla C (2008) *Metabolismo of nicotinamide,adenine and inosine in developing microspore-derived canola (Brassica napus) embryos.* Plant Physiol and Biochem 46:752-759;

Azevedo BR, (1996) *Cancro Cronologia histórica e Génese de ideias*. Faculdade de Medicina de Coimbra Instituto de Patologia Geral 31-32;

Bayet-Robert M, Lim S, Barthomeuf C and Morvan D (2010) *Biochemical disorders induced by cytotoxic marine natural products in breast cancer cells as revealed by proton NMR spectroscopy-based metabolomics*. Biochem Pharmacol 80:1170-1179;

Berners-Prince SJ, Ronconi L, Sadler PJ (2006) *Insights into the mechanism of platinum anticancer drugs from multinuclear NMR spectroscopy*. Progress in Nuclear Magnetic Reson Spect 49:65-98;

Bernardo B (1982) *Citogenética Humana*. Guanabara Koogan 63-64;

Bezabeh T, Mowat MR, Jarolim L, Greenberg A and Smith I (2001) *Detection of drug-induced apoptosis and necrosis in human cervical carcinoma cells using ^{1}H NMR spectroscopy*. Cell Death and Differ 8:219-224;

Boffetta P (2006) *Human Cancer from environmental pollutants: the epidemiological evidence.* Mutat Res 608:157-162;

Brabletz S and Brabletz T (2010) *The ZEB/miR-200 feedback loop—a motor of cellular plasticity in development and cancer?.* Europ Molec Biol Org 11:670-667;

Carloni P and Alber F (2003) *Quantum Medicinal Chemistry.* Wiley-VCH 124-141;

Cataldi A, Giocomo V, Rapino S and Rana R *Ionizing Radiation Induces Apoptotic Signal Through Protein Kinase Cδ (delta) and Survival Signal Through Akt and Cyclic-Nucleotide Response Element- Binding Protein (CREB) in Jurkat T Cells.* Biol Bull 217:202-212;

Centerwall C, Kerwood D, Goodisman J, Toms B and Dabrowiak J (2008) *New extracellular resistance mechanism for cisplatin*. J of Inorg Biochem 102:1044-1049;

Chen J, Xing MMQ and Zhong W (2011) *Degradable micelles based on hydrolytically degradable amphiphilic graft copolymers for doxorubicin delivery*. Polymer 52:933-941;

Claridge T (1999) *High-Resolution NMR Techniques in Organic Chemistry* Pergamon vol 9;

Cox I, Sharif A, Cobbold J, Thomas H and Taylor-Robinson S (2006) *Current and future applications of in vitro magnetic resonance spectroscopy in hepatobiliary disease*. World J Gastro 12: 4773-4783;

Croce CM (2008 a) *Molecular Origins of Cancer Oncogenes and Cancer*. N Eng J M 358:502-511;

Croce CM (2008 b) *Oncogenes and cancer.* Review Article N Engl J M 358:502-11;

Čuperlović-Culf M, Barnett D, Culf A and Chute I (2010) *Cell culture metabolomics: applications and future directions.* Drug Discov Today 15:610-621;

Daly PF, (1988) *^{31}P-NMR spectroscopy of human cancer cells proliferating in a basement membrane gel*. FASEB J. 2:2596-2604;

Davies M, Berners-Prince S and Hambley T (1998) *Rates of platination of AG and GA containing double-stranded oligonucleotides: Insights into why Cisplatin binds to GG and AG but not GA sequences in DNA.* J Am Chem Soc 120:11380-11390;

Davies M, Berners-Prince S and Hambley T (2000 a) *Rates of platination of –AG- and –GA-containing double-stranded oligonucleotides: effect of chloride concentration*. J of Inorg Biochem 79:167-172;

Davies M, Berners-Price S and Hambley T (2000 b) *Slowing of Cisplatin Aquation in the Presence of DNA but not in the Presence of Phosphate: Improved Understanding of Sequence Selectivity and the Roles of Monoaquated and Diaquated Species in the Binding of Cisplatin to DNA.* Inorg Chem 39:5603-5613;

DeVita H and Rosenberg S (2005) *Cancer. Principles & Practice of Oncology. Lippincott Williams, Philadelphia USA*;

Duarte I, Lamego I, Rocha C and Gil A (2009 a) *NMR metabonomics for mammalian cell metabolism studies* Bioanal 1:1597–1614;

Duarte I, Marques J, Ladeirinha A, Rocha C, Lamego I, Calheiros R, SilvaT,. Marques M, Melo J, Carreira I and Gil A (2009 b) *Analytical Approaches toward Successful Human Cell Metabolome Studies by NMR Spectroscopy*. Anal Chem 81:5023-5032;

Duarte I, Lamego I, Marques J, Marques M, Blaise B and Gil A (2010) *Nuclear Magnetic Resonance (NMR) Study of the Effect of Cisplatin on the Metabolic Profile of MG-63 Osteosarcoma Cells*. J of Prot Resear 9:5877-5886;

Dubey S and Powell C (2008) *Update in Lung Cancer*. Am J Respir Crit Care Med 177: 941- 946;

Durovic B, Selakovic V and Spasic-Jokic V (2004) *Does occupational exposure to low-dose ionizing radiation induce cell membrane damage?.* Arch Oncol 12:197-199;

El-Khateeb M, Appleton T, Gahan L, Charles B, Berners-Price S and Bolton A (1999) *Reactions of cisplatin hydrolytes with methionine, cysteine, and plasma ultrafiltrate studied by a combination of HPLC and NMR techniques*. J of Inorg Biochem 77:13-21;

Gil V, Geraldes M and Carlos F (1987) *Ressonância Magnética Nuclear Fundamentos e Aplicações.* Fund Caloust Gulbenk Lisboa;

Gomes J (2007) *Estabelecimento e caracterização in vitro e in vivo de linhas celulares de tumores da mama de cadela.* Tese de Mestrado em Medicina e Oncologia Molecular da Universidade de Medicina do Porto;

Griffin J and Shockcor J (2004) *Metabolic Profiles of cancer cells.* N Rev 4:551-561;

Griffin J and Kauppinen R (2007) A *metabolomics perspective of human brain tumours.* FEBS J 274:1132-1139;

Hendrich and Michalak (2003) *Lipids as a target for drugs modulating multidrug resistance of cancer cells.* Curret Drug Target 4:23-30;

Huang Z, Tong Y, Wang J and Huang Y (2003) *NMR studies of the relationship between the changes of membrane lipids and the cisplatin-resistance of A549/DDP cells.* C Cell Int 3:1-8;

Jansen J, Hakumaki J, Ifeanyi L, Shamblott M, Gearhart J and van Zijl P (2002) *^{1}H-NMR spectroscopy of stem cells in vitro demonstrates high proliferation state.* Mag Reson Med 10:1-10;

Khool SHG and Al-Rubeai M (2007) *Metabolomics as a complementary tool in cell culture* Biotechnol. Appl Biochem 47:71–84;

Kim C, Kim J, Nam S, Yang K, Jeong M, Kim H, Lim Y, Kim C, Jin Y and Kim J (2007) *Low-dose of Ionizing radiation enhances cell proliferation via transient ERK1/2 and p38 activation in normal lung fibroblasts*. J Radiat Res 48:407-415;

Lam A, Lam S, Lai K, Tong T and Chau T (2006). *High rate of detection of subtelomeric aberration by using combined MLPA and subtelomeric FISH approach in patients with moderate to severe mental retardation*. Clin Biochem 39: 196-202;

Liang X, So Y, Cui J, Ma K, Xu X, Zhao Y, Cai L and Li W (2011) *The low-dose Ionizing Radiation stimulates cell proliferation via activation of the MAPK/ERK Pathway in rat cultured mesenchymal stem cells.* J of Radiat Resear 52:380-386);

Lião L, Choze R, Cavalcante P, Santos S, Ferri P and Ferreira A (2010) *Perfil Químico de Cultivares de feijão (Phaseolus vulgaris) pela Técnica de High Resolution Magic Angle Spinning (HRMAS)*. Quim Nova 33:634-638;

Lindon J, Holmes E, Bollard M, Stanley E and Nicholson J (2004) *Metabonomics technologies and their applications in physiological monitoring, drug safety assessment and disease diagnosis. Biomarkers.* Biomark Rev 9:1-31;

Lindon J and Nicholson J (2008) *Spectroscopic and Statistical Techniques for Information Recovery in Metabonomics and Metabolomics.* Annu Rev Anal Chem1:45-69;

Lodish H, Berk A, Matsudaira P, Kaiser C, Krieger M, Scott M, Zipursky L and James Darnell (2004) *Molecular Cell Biology*. 5º edition 935-973;

Luciani A, Grande S, Palma A, Rosi A, Giovannini C, Sapora O, Viti V and Guidoni L (2009) *Characterization of ^{1}H NMR detectable mobile lipids in cells from human adenocarcinomas.* FEBS J 276:1333-1346;

Ludwig C, Ward D, Martin A, Viant M, Ismail T, Johnson P, Wakelam M and Günther U (2009) *Fast targeted multidimensional NMR metabolomics of colorectal cancer.* Magnetic Reson in Chem 47:68-73;

Mahmood U, Alfieri A, Thaler H, Cowburn D and Koutcher J (1994) *Radiation dose-dependent changes in tumor metabolism measured by ^{31}P nuclear magnetic resonance spectroscopy*. Canc Resear 54:4885-4891;

Marekova M, Vávrová J, Vokurková D and Psutka J (2003) *Modulation of Ionizing Radiation-Induced Apoptosis and Cell Cycle Arrest by All-Trans Retinoic Acid in Promyelocytic Leukemia Cell (HL-60)* Physiol Res 52:599-606;

Matés J, Pérez-Gómez C, Núñez de Castro I, Asenjo M and Márquez J (2002) *Glutamine and its relationship with intracellular redox status, oxidative stress and cell proliferation/death.* The Internat J of Biochem and Cell Biol 34:439-458;

Matulewicz L, Cicho A, Jurkowski M, Przybyszewski W, Gibas M and Sokó M (2006) *Response to D_0 dose of ionizing radiation of C6 glioma cell line measured by high resolution ^{1}H NMR spectroscopy*. Polish J of Environ Stud 15:188-190;

Merz A and Serkova N (2009) *Use of nuclear magnetic resonance-based metabolomics in detecting drug resistance in cancer*. Biomark Med 3: 289-306;

Mochizuki T, Ishii G, Nagai K, Yoshida J, Nishimura M, Mizuno T, Yokose T, Suzuki K and Ochiai A (2008) *Pleomorphic Carcinoma of the Lung Clinicopathologic Characteristics of 70 Cases.* Am J Surg Pathol 32:1727–1735;

Nascimento C and Bloch (2001) *Ressonância Magnética Nuclear: Gradus Primus.* Biotec Cienc e Desenv 21:52-61;

Norton L and Layman D (2006) *Leucine Regulates Translation Initiation of Protein Synthesis in Skeletal Muscle after Exercise.* The J of nutrit 136:533S-S537;

Parkin D, Bray F, Ferlay J and Pisani P (2005) *Global Cancer Statistics*. CA C J Clin 55:74-108;

Parthymou A, Kardamakis D, Pavlopoulos I and Papadimitriou E (2004) *Irradiated C6 glioma cells induce angiogenesis in vivo and activate endothelial cells in vitro.* Int J C 110:807-814;

Patrinos G and Ansorge W (2005) *Molecular diagnostics*. Academic Press;

Pitot H (1993) *The Molecular Biology of Carcinogenesis*. Cancer 72:962-70;

Pollock R, Doroshow J, Khayat D, Nakao A and O'Sullivan B (2006) *Manual de Oncologia Clínica da UICC*. Wiley 8° edição;

Puthran S, Sudha K, Rao G and Shetty B (2009) *Oxidative stress and low dose ionizing radiation.* Ind J Physiol Pharmacol 53:181-184;

Reynolds P, Allison C and Willnauer C (2010) *TTF-1 regulates a5 nicotinic acetylcholine receptor (nAChR) subunits in proximal and distal lung epithelium.* Respirat Resear 11:1-10;

Reeder F, Guo Z, Murdoch PD, Corazza A, Hambley T, Berners-Price S, Chottard J and Sadler P (1997) *Platination of a GG site on single-stranded and double-stranded forms of a*

14-base oligonucleotide with diaqua cisplatin followed by NMR and HPLC – Influence of the platinum ligands and sequence on 5'-G versus 3'-G platination selectivity. Euro J Biochem 249:370-382;

Reedijk J (2009) *Platinum Anticancer Coordination Compounds: Study of Binding Inspires New Drug Design.* Eur J Chem 1:1303-1312;

Reid ME, Santella R and Ambrosone C (2008) Molecular Epidemiology to Better Predict Lung Cancer Risk. Clin Lung C 3:149 – 153;

Robertis E and Robertis E (1987) *Cell and Molecular Biology*. 8º edition;

Santini M, Romano R, Rainaldi G, Indovina P, Ferrante A, Motta A and Indovina P (2006 a) *Temporal Dynamics of 1H-NMR-Visible Metabolites during Radiation-Induced Apoptosis in MG-63 Human Osteosarcoma Spheroids.* Rad Resear 166: 734-745;

Santini M, Romano R, Rainaldi G, Ferrante A, Indovina P, Motta A and Indovina P (2006) *^{1}H-NMR Evidence for a Different Response to the Same Dose (2 Gy) of Ionizing Radiation of MG-63 Human*. Anic resear 26:267-282);

Santoro E (2005) *The history of gastric cancer: legends and chronicles.* Gastric C 8:71-74;

Sellem D, Elbayed K, Neuville A, Moussallieh F, Lang-Averous G, Piotto M, Bellocq J and Namer I (2011) *Metabolomic Characterization of Ovarian Epithelial Carcinomas by HRMAS-NMR Spectroscopy.* J of Oncol 2011:1-9;

Shanaiah N, Zhang S, Desilva M and Raftery D (2008) *NMR-based metabolomics for biomarker discovery*. Met in Pharmacol and Toxicol 10:341-368;

Siddik Z (2003) *Cisplatin: mode of cytotoxic action and molecular basis of resistance.* Oncog 22:7265-7279;

Sitter B, Bathen T, Tessem M and Gribbestad I (2009) *High-resolution magic angle spinning (HR MAS) MR spectroscopy in metabolic characterization of human cancer.* Prog in Nucl Res Spect 10:1-16;

Stenman K, Stattin P, Stenlund H, Riklund K, Gröbner G and Bergh A (2011) *^{1}H HRMAS NMR Derived Bio-markers Related to Tumor Grade, Tumor Cell Fraction, and Cell Proliferation in Prostate Tissue Samples*. Biomar Insight 6:39-47;

Sun S, Schiller J and Gazdar A (2007) *Lung Cancer in Never Smokers - A Different disease.* Nat Rev 7:778 – 790;

Suzuki K, Kodama S and Watanabe M (2001) *Extremely Low-Dose Ionizing Radiation Causes Activation of Mitogen-activated Protein Kinase Pathway and Enhances Proliferation of Normal Human Diploid Cells.* C Resear 61:5396-5401;

Tiziani S, Lopes V and Gunther U (2009 a) *Early Stage Diagnosis of Oral Cancer Using ^{1}H NMR-based Metabolomics*. Neoplasia 11:269-276;

Tiziani S, Lodi A, Khanim F, Viant M, Bunce C and Günther U (2009 b) *Metabolomic Profiling of Drug Responses in Acute Myeloid Leukaemia Cell Lines*. PloS ONE 4:1-10;

Tucker J (2008) *Low-dose ionizing radiation and chromosome translocations: A review of the major considerations for human biological dosimetry.* Mut Resear 659:211-220;

Vianna D, Teodoro G, Torres-Leal F and Tirapegui J (2010) *Protein synthesis regulation by leucine.* Braz J of Pharmac Scienc 46:29-36;

Vinje J and Sletten E (2007) *NMR Spectroscopy of Anticancer Platinum Drugs*. Anti-cancer Agents in Med Chem 7:35-54;

Vincent TL and Gatenby RA (2008) *An evolutionary model for initiation, promotion, and progression in carcinogenesis*. Inter J of Oncol 32:729-737;

Wang X, Du X, Li H, Chan D and Sun H (2011) *The Effect of the Extracellular Domain of Human Copper Transporter (hCTR1) on Cisplatin Activation*. Chem Int Ed 50:2706-2711;

Wang Z, Li Y, Kong D, Banerjee S, Ahmad A, Azmi A, Ali S, Abbruzzese J, Gallick G and Sarkar F (2009) *Acquisition of epithelial–mesenchymal transition phenotype of gemcitabine-*

resistant pancreatic cancer cells is linked with activation of the notch signaling pathway. Canc Res 69:2400–2407;

Wider G (2002) *High-resolution nuclear magnetic resonance applied to biophysics and molecular biology: highlights and challenges.* IEEE Transactions on Applied Superconductivity volume 12:740-745;

Wishart D (2008) *Quantitative metabolomics using NMR*. Trends in Anal Chem 27:228-237;

Wu R (2004) *Growth of Human Lung Tumor Cells in Culture*. Culture of Human Tumor Cells;

Xiao D and He J (2010) *Epithelial mesenchymal transition and lung cancer*. J Thorac Dis 2010; 2: 154-159;

Zira A, Theocharis S, Mitropoulos D, Migdalis V and Mikros E (2010) *^{1}H NMR Metabonomic Analysis in Renal Cell Carcinoma: a Possible Diagnostic Tool*. J of Prot Resear 9:4038-4044;

http://nobelprize.org/nobel_prizes/medicine/laureates/1931/index.html;

http://evunix.uevora.pt/~sinogas/TRABALHOS/2001/Imuno01_desord_linfo.htm;

http://www.proximus.com.br/news/content/suplementacao_com_l_glutamina_e_desempenho_fisico;

http://www.atcc.org/ATCCAdvancedCatalogSearch/ProductDetails/tabid/452/Default.aspx?ATCCNum=CCL-185&Template=cellBiology